European Journal of Mechanics B/Fluids 28 (2009) 170–184

Contents lists available at ScienceDirect

European Journal of Mechanics B/Fluids

www.elsevier.com/locate/ejmflu

Model Boltzmann equation for gas mixtures: Construction and numerical comparison

Shingo Kosuge

Department of Mechanical Engineering and Science and Advanced Research Institute of Fluid Science and Engineering, Graduate School of Engineering, Kyoto University, Kyoto 606-8501, Japan

ARTICLE INFO

Article history:
Received 9 January 2008
Received in revised form 25 April 2008
Accepted 5 May 2008
Available online 22 May 2008

PACS:
51.10.+y
05.20.Dd
47.45.-n
47.70.Nd

Keywords:
Boltzmann equation
Kinetic theory of gases
Rarefied gas dynamics
Molecular gas dynamics
Kinetic model
Gas mixture

ABSTRACT

A new model for the nonlinear Boltzmann equation for gas mixtures is constructed by the method employed in the derivation of the McCormack model in the linearized kinetic theory [F.J. McCormack, Phys. Fluids 16 (1973) 2095]. Then it is compared numerically with other existing models proposed in [P. Andries, K. Aoki, B. Perthame, J. Stat. Phys. 106 (2002) 993] and in [L.H. Holway Jr., Phys. Fluids 9 (1966) 1658] (the so-called ES-BGK model) as well as with the original Boltzmann equation. The new model is not restricted to the Maxwell molecule, can fit to general molecular models, and reproduces well solutions of the Boltzmann equation at least in the case of weak nonequilibrium. The numerical comparison is performed in the case of a binary gas mixture consisted of the hard-sphere or pseudo Maxwell molecules, after parameters concerning the molecular interaction are adjusted appropriately.

1. Introduction

It is well known that rarefied gases, in which the molecular mean free path is not negligible compared to the typical scale of the flow, should be dealt with not by the system of conventional fluid-dynamic equations but by the Boltzmann equation. The analysis of the latter equation is, however, not an easy task, mainly because of the complexity of the collision term, which represents effects of molecular interactions on a change of the velocity distribution function of molecules. Therefore, most of the numerical analyses are performed usually by the use of the direct simulation Monte Carlo (DSMC) method [1], where the behavior of a gas is approximated by movements and collisions of a small number of simulation particles, or by the use of the model Boltzmann equation such as the BGK (or BKW) [2,3] or ES-BGK [4–6] model, where the complex collision term is replaced by simpler model so that some essential properties of the original collision term are retained as far as possible.

Although the DSMC method can be rather easily applied to wide variety of problems including the complex geometry, chemical reactions, etc., the results are inevitably suffered from the statistical scatter because of the probabilistic nature of the method. On the other hand, accurate solutions of the model equation are obtainable by means of deterministic computational methods such as a finite-difference method. However, since it is nothing but a model, the question whether the solutions of the model equation are close to the corresponding solutions of the original Boltzmann equation would arise. In the case of a single-component gas, numerical comparisons between the Boltzmann equation and its models (BGK, ES-BGK, and their extensions) were made recently in Refs. [7–10] and, as a result, the excellent agreement was found in some cases where the models with the correct Prandtl number (or the viscosity and thermal conductivity) were employed.

After the invention of the BGK model for single-component gases, considerable efforts have been devoted also to the construction of model equations for the practically more important case of gas mixtures [11–18]. The agreement between results of the Boltzmann equation and those of models in this case is expected to be more difficult to achieve, since additional physical effects will be brought about by cross collisions (collisions between molecules of different component species). Previously in Ref. [19], we compared numerically the Boltzmann equation with the model proposed by Hamel [14], that by Garzó, Santos, and Brey [17] and that by An-

E-mail address: kosuge@aero.mbox.media.kyoto-u.ac.jp.

0997-7546/$ – see front matter
doi:10.1016/j.euromechflu.2008.05.001

dries, Aoki, and Perthame [18] in the case of a binary mixture of the Maxwell molecular gases. Roughly speaking, solutions of the above three models compared in Ref. [19] behaved in similar fashion and the resemblance to solutions of the Boltzmann equation was insufficient: since parameters concerning the molecular interaction contained in the models were adjusted so that the mutual diffusion coefficient takes the correct value, the other transport coefficients (i.e., the viscosity and thermal conductivity) were generally not correct and profiles of flow velocity and temperature obtained by the models did not agree well with those by the Boltzmann equation (see Ref. [19] for details).

The purpose of this paper is to construct a new model equation for mixtures and to make the numerical comparison similar to those reported in Ref. [19] including the new model and other existing models. The collision term of the new model approximates the original one of the Boltzmann equation by the use of a polynomial in the molecular velocity, whose coefficients are determined by the method of *equivalence of moment*. This method was employed in the derivation of the McCormack model [20] in the linearized kinetic theory. Therefore we shall call the new model *the polynomial model* in the following. As in the case of the McCormack model, the polynomial model is not restricted to the Maxwell molecule but can fit to the general molecular models. The numerical comparison is first performed among the original Boltzmann equation, the polynomial model, the mixture version of the ES-BGK model [4,5], and the Andries et al.'s model in the case of the Maxwell molecule. We can expect that the ES-BGK and polynomial model may reproduce solutions of the Boltzmann equation better than the Andries et al.'s model (and the other models studied in Ref. [19]) does, because of the reason which will be clear subsequently. Then, the comparison in the case of the hard-sphere molecule is performed only between the Boltzmann equation and the polynomial model, since the other two models are basically appropriate only for the Maxwell molecular gases. By the way, the gas separation effect in the thermally induced flow of a binary mixture was investigated recently in Refs. [21,22] and the Maxwell molecule was found to be incapable of describing the effect (this incapability cannot be fully explained by the well-known fact that the Maxwell molecule does not reproduce the thermal diffusion [23]; see Ref. [21]). The above findings in Refs. [21,22] indicate that the usage of the general molecular models other than the Maxwell molecular model could be sometimes crucial in analyses of the behavior of gas mixtures.

The paper is organized as follows. In Section 2, the Boltzmann equation for mixtures is introduced and some quantities which will be used to make a proper comparison with the model equations are calculated in the case of the Maxwell molecule. Two existing model equations, i.e., the Andries et al.'s model and ES-BGK model, are introduced in Section 3.1 and the new polynomial model is constructed in Section 3.2. Then, the numerical comparison is performed in Section 4.1 in the case of the Maxwell molecule and in Section 4.2 in the case of the hard-sphere molecule. We conclude the paper in Section 5.

2. Boltzmann equation

In this paper, the Greek letters α, β, and γ will be used symbolically to indicate the component species of gas mixture. Let t be the time, X_i (or $\boldsymbol{X}$) the space rectangular coordinate, ξ_i (or $\boldsymbol{\xi}$) the molecular velocity, $f^\alpha(t, \boldsymbol{X}, \boldsymbol{\xi})$ the velocity distribution function of α-species molecules. The Boltzmann equation for a gas mixture in the absence of the external force may be written as

$$\frac{\partial f^\alpha}{\partial t} + \xi_j \frac{\partial f^\alpha}{\partial X_j} = \sum_\beta J^{\beta\alpha}(f^\beta, f^\alpha), \tag{1}$$

where, and in the sequel, the summation with respect to β (indicating the component species) is taken over the whole gas species. The collision term $J^{\beta\alpha}$ may be expressed as

$$J^{\beta\alpha}(f,g) = \int \left[f(\boldsymbol{\xi}_*^{\beta\alpha}) g(\boldsymbol{\xi}^{\beta\alpha}) - f(\boldsymbol{\xi}_*) g(\boldsymbol{\xi}) \right] \times B^{\beta\alpha}\left(\frac{|\boldsymbol{e}\cdot\boldsymbol{V}|}{|\boldsymbol{V}|}, |\boldsymbol{V}| \right) \mathrm{d}\Omega(\boldsymbol{e})\, \mathrm{d}^3\xi_*, \tag{2a}$$

$$\boldsymbol{\xi}^{\beta\alpha} = \boldsymbol{\xi} + \frac{\mu^{\beta\alpha}}{m^\alpha}(\boldsymbol{e}\cdot\boldsymbol{V})\boldsymbol{e}, \qquad \boldsymbol{\xi}_*^{\beta\alpha} = \boldsymbol{\xi}_* - \frac{\mu^{\beta\alpha}}{m^\beta}(\boldsymbol{e}\cdot\boldsymbol{V})\boldsymbol{e}, \tag{2b}$$

$$\boldsymbol{V} = \boldsymbol{\xi}_* - \boldsymbol{\xi}, \qquad \mu^{\beta\alpha} = \frac{2m^\beta m^\alpha}{m^\beta + m^\alpha}. \tag{2c}$$

Here m^α is the molecular mass of species α, $\boldsymbol{e}$ a unit vector, $\mathrm{d}\Omega(\boldsymbol{e})$ the solid angle element in the direction of $\boldsymbol{e}$, and $\mathrm{d}^3\xi_* = \mathrm{d}\xi_{*1}\,\mathrm{d}\xi_{*2}\,\mathrm{d}\xi_{*3}$. The integration in Eq. (2a) is carried out over the whole space of $\boldsymbol{\xi}_*$ and the whole direction of $\boldsymbol{e}$. The domain of integration appearing in the sequel is, unless otherwise stated, the whole space of the integration variables. The $B^{\beta\alpha}$ $(= B^{\alpha\beta})$ is a nonnegative function, whose functional form is determined by the intermolecular force between species β and α. Specific forms of $B^{\beta\alpha}$ for the hard-sphere (HS) and Maxwell molecules will be shown later in this section.

The macroscopic quantities such as the molecular number density n^α, flow velocity v_i^α, pressure p^α, temperature T^α, stress tensor p_{ij}^α, and heat-flow vector q_i^α of species α are defined in terms of the moments of f^α:

$$\begin{aligned}
&n^\alpha = \int f^\alpha\, \mathrm{d}^3\xi, \qquad v_i^\alpha = \frac{1}{n^\alpha}\int \xi_i f^\alpha\, \mathrm{d}^3\xi,\\
&p^\alpha = kn^\alpha T^\alpha = \frac{1}{3}\int m^\alpha |\boldsymbol{\xi} - \boldsymbol{v}^\alpha|^2 f^\alpha\, \mathrm{d}^3\xi,\\
&p_{ij}^\alpha = \int m^\alpha (\xi_i - v_i^\alpha)(\xi_j - v_j^\alpha) f^\alpha\, \mathrm{d}^3\xi,\\
&q_i^\alpha = \frac{1}{2}\int m^\alpha (\xi_i - v_i^\alpha)|\boldsymbol{\xi} - \boldsymbol{v}^\alpha|^2 f^\alpha\, \mathrm{d}^3\xi,
\end{aligned} \tag{3}$$

with k being the Boltzmann constant and $\mathrm{d}^3\xi = \mathrm{d}\xi_1\,\mathrm{d}\xi_2\,\mathrm{d}\xi_3$. The molecular number density n, flow velocity v_i, pressure p, temperature T, stress tensor p_{ij}, and heat-flow vector q_i of the total mixture are written in terms of those of the component species as

$$\begin{aligned}
&n = \sum_\beta n^\beta, \qquad v_i = \left(\sum_\beta \rho^\beta v_i^\beta\right) \Big/ \left(\sum_\beta \rho^\beta\right),\\
&p = knT = \sum_\beta \left(p^\beta + \frac{1}{3}\rho^\beta |\boldsymbol{v}^\beta - \boldsymbol{v}|^2 \right),\\
&p_{ij} = \sum_\beta \left[p_{ij}^\beta + \rho^\beta (v_i^\beta - v_i)(v_j^\beta - v_j) \right],\\
&q_i = \sum_\beta \left[q_i^\beta + p_{ij}^\beta (v_j^\beta - v_j) + \frac{3}{2} p^\beta (v_i^\beta - v_i) \right.\\
&\qquad \left. + \frac{1}{2}\rho^\beta (v_i^\beta - v_i)|\boldsymbol{v}^\beta - \boldsymbol{v}|^2 \right],
\end{aligned} \tag{4}$$

with ρ^α $(\equiv m^\alpha n^\alpha)$ being the mass density of species α.

Let us now show specific forms of the function $B^{\beta\alpha}$ appearing in the collision term (2a) for the HS and Maxwell molecules. In the case of the HS molecules, it is written as (see Refs. [24,21])

$$B^{\beta\alpha} = \frac{(d^{\beta\alpha})^2}{2}|\boldsymbol{e}\cdot\boldsymbol{V}|, \qquad d^{\beta\alpha} = \frac{d^\beta + d^\alpha}{2}, \tag{5}$$

with d^α being the molecular diameter of species α. In the case of the Maxwell molecules, the potential $U^{\beta\alpha}$ of the intermolecular force between β- and α-species molecules are given by

$U^{\beta\alpha} = a^{\beta\alpha} r^{-4}$ with r being the distance between the centre of the molecules and $a^{\beta\alpha}$ $(= a^{\alpha\beta})$ a positive constant. The $B^{\beta\alpha}$ in this case is written as (see Refs. [24,21])

$$B^{\beta\alpha} = \left(\frac{a^{\beta\alpha}}{\mu^{\beta\alpha}}\right)^{1/2} \frac{g(\theta)}{\sin\theta}\frac{\mathrm{d}g}{\mathrm{d}\theta}, \qquad 0 \leqslant \theta \ \left(\equiv \arccos\left(|\boldsymbol{e}\cdot\boldsymbol{V}|/|\boldsymbol{V}|\right)\right) < \frac{\pi}{2}, \tag{6}$$

where g is a monotonically increasing function of θ and is defined by the following integral:

$$\theta = \int_0^{y_c(g)} \left[1 - (y/g)^4 - y^2\right]^{-1/2} \mathrm{d}y, \qquad y_c = \left[\frac{-g^4 + (g^8 + 4g^4)^{1/2}}{2}\right]^{1/2}. \tag{7}$$

Note that $g(0) = 0$ and $g(\pi/2) = \infty$. It should be also noted that $B^{\beta\alpha}$ in Eq. (6) is a function of θ only and is independent of the magnitude of the relative velocity $|\boldsymbol{V}|$ of colliding molecules. In the following, however, we introduce the so-called angular cutoff, setting $B^{\beta\alpha} = 0$ for $\theta_c^{\beta\alpha} \leqslant \theta \leqslant \pi/2$ where $\theta_c^{\beta\alpha}$ is a constant, which corresponds to ignoring the contribution of the grazing collisions in the neighborhood of $\theta = \pi/2$. The reason of this is because we need a definite value of the molecular collision frequency [defined later in Eq. (8) in the next subsection] in order to make a proper comparison between the Boltzmann and its model equations (see Section 4). The Maxwell molecule with the cutoff is called the *pseudo Maxwell molecule* (see, e.g., Ref. [25]).

In this paper, we will make numerical comparisons between the original Boltzmann equation for the HS and pseudo Maxwell molecules and the model Boltzmann equations in the case of binary mixtures. Before introducing the model equations in Section 3, we shall compute the molecular collision frequency and moments of the collision term for the pseudo Maxwell molecules in the next subsection, since those quantities will be used to make proper comparisons in Section 4.

2.1. Collision frequency and moments of the collision term for the pseudo Maxwell molecules

Let us define the collision frequency $\nu^{\beta\alpha}(\boldsymbol{\xi})$ of an α-species molecule with velocity $\boldsymbol{\xi}$ with respect to collisions with β-species molecules by the following integral:

$$\nu^{\beta\alpha}(\boldsymbol{\xi}) = \int f^{\beta}(\boldsymbol{\xi}_*) B^{\beta\alpha}\left(\frac{|\boldsymbol{e}\cdot\boldsymbol{V}|}{|\boldsymbol{V}|}, |\boldsymbol{V}|\right) \mathrm{d}\Omega(\boldsymbol{e})\,\mathrm{d}^3\xi_*. \tag{8}$$

Substituting Eq. (6) with the angular cutoff into the above definition, we see that $\nu^{\beta\alpha}$ for the pseudo Maxwell molecule does not depend on $\boldsymbol{\xi}$ and is given by

$$\nu^{\beta\alpha} = K^{\beta\alpha} n^{\beta}, \tag{9a}$$

$$K^{\beta\alpha} = 2\pi\left(a^{\beta\alpha}/\mu^{\beta\alpha}\right)^{1/2}\left(g_c^{\beta\alpha}\right)^2, \qquad g_c^{\beta\alpha} = g\left(\theta_c^{\beta\alpha}\right). \tag{9b}$$

We next compute moments of the collision term (2a). The following notation will be used:

$$\left\langle h(\xi_i)\right\rangle_{\beta\alpha} \equiv \int h(\xi_i) J^{\beta\alpha}\left(f^{\beta}, f^{\alpha}\right)\mathrm{d}^3\xi. \tag{10}$$

In the case of the (pseudo) Maxwell molecule, one can obtain the following results without specific knowledge of the velocity distribution functions [26]:

$$\left\langle m^{\alpha}\boldsymbol{\xi}\right\rangle_{\beta\alpha} = \chi^{\beta\alpha}\mu^{\beta\alpha} n^{\beta} n^{\alpha}\left(\boldsymbol{v}^{\beta} - \boldsymbol{v}^{\alpha}\right), \tag{11a}$$

$$\left\langle \frac{m^{\alpha}}{2}|\boldsymbol{\xi}|^2\right\rangle_{\beta\alpha} = \chi^{\beta\alpha}\frac{\mu^{\beta\alpha} n^{\beta} n^{\alpha}}{m^{\beta} + m^{\alpha}}\left[3k\left(T^{\beta} - T^{\alpha}\right) + \left(m^{\beta}\boldsymbol{v}^{\beta} + m^{\alpha}\boldsymbol{v}^{\alpha}\right)\cdot\left(\boldsymbol{v}^{\beta} - \boldsymbol{v}^{\alpha}\right)\right], \tag{11b}$$

with

$$\chi^{\beta\alpha} = 2\pi\left(a^{\beta\alpha}/\mu^{\beta\alpha}\right)^{1/2} A\left(g_c^{\beta\alpha}\right), \qquad A(z) = 2\int_0^z g\cos^2\theta\,\mathrm{d}g. \tag{12}$$

Eqs. (11a) and (11b) represent, respectively, the collisional transfer of momentum and that of energy between species β and α per unit time and per unit volume. Note that the coefficient $\chi^{\beta\alpha}$ defined in Eq. (12) has its meaning only for $\beta \neq \alpha$, since the collisional transfer of momentum and that of energy between like molecules are identically zero in total [see Eq. (11) with $\beta = \alpha$].

Furthermore, one can obtain the following results for higher-order moments of the collision term in the case of the (pseudo) Maxwell molecule [27]:

$$\begin{aligned}
&\left\langle m^{\alpha}\overline{c_i^{\alpha} c_j^{\alpha}}\right\rangle_{\beta\alpha} \\
&\quad = \chi^{\beta\alpha}\frac{2\mu^{\beta\alpha} n^{\beta} n^{\alpha}}{m^{\beta} + m^{\alpha}}\left[\frac{\overline{p_{ij}^{\beta}}}{n^{\beta}} - \frac{\overline{p_{ij}^{\alpha}}}{n^{\alpha}} + m^{\beta}\overline{\left(v_i^{\beta} - v_i^{\alpha}\right)\left(v_j^{\beta} - v_j^{\alpha}\right)}\right] \\
&\qquad - \eta^{\beta\alpha}\frac{\mu^{\beta\alpha}\rho^{\beta} n^{\alpha}}{m^{\beta} + m^{\alpha}}\left[\frac{\overline{p_{ij}^{\beta}}}{\rho^{\beta}} + \frac{\overline{p_{ij}^{\alpha}}}{\rho^{\alpha}} + \overline{\left(v_i^{\beta} - v_i^{\alpha}\right)\left(v_j^{\beta} - v_j^{\alpha}\right)}\right],
\end{aligned} \tag{13a}$$

$$\begin{aligned}
&\left\langle \frac{m^{\alpha}}{2} c_i^{\alpha}|\boldsymbol{c}^{\alpha}|^2\right\rangle_{\beta\alpha} \\
&\quad = \chi^{\beta\alpha}\frac{4\mu^{\beta\alpha}\rho^{\beta} n^{\alpha}}{(m^{\beta} + m^{\alpha})^2}\left\{\frac{q_i^{\beta}}{n^{\beta}} - \frac{(m^{\beta})^2 + 3(m^{\alpha})^2}{4m^{\beta}m^{\alpha}}\frac{q_i^{\alpha}}{n^{\alpha}}\right. \\
&\qquad + \left(v_j^{\beta} - v_j^{\alpha}\right)\left[\frac{\overline{p_{ij}^{\beta}}}{n^{\beta}} + \frac{(m^{\beta} - m^{\alpha})^2}{4m^{\beta}m^{\alpha}}\frac{\overline{p_{ij}^{\alpha}}}{n^{\alpha}}\right] \\
&\qquad \left. + \frac{v_i^{\beta} - v_i^{\alpha}}{2}\left[5kT^{\beta} + \frac{5(m^{\beta} - m^{\alpha})^2}{4m^{\beta}m^{\alpha}}kT^{\alpha} + m^{\beta}\left|\boldsymbol{v}^{\beta} - \boldsymbol{v}^{\alpha}\right|^2\right]\right\} \\
&\qquad - \eta^{\beta\alpha}\frac{4\mu^{\beta\alpha}\rho^{\beta} n^{\alpha}}{3(m^{\beta} + m^{\alpha})^2}\left\{\frac{q_i^{\beta}}{n^{\beta}} + \frac{q_i^{\alpha}}{n^{\alpha}}\right. \\
&\qquad + \left(v_j^{\beta} - v_j^{\alpha}\right)\left(\frac{\overline{p_{ij}^{\beta}}}{n^{\beta}} + \frac{3m^{\beta} - m^{\alpha}}{4m^{\alpha}}\frac{\overline{p_{ij}^{\alpha}}}{n^{\alpha}}\right) \\
&\qquad \left. + \frac{v_i^{\beta} - v_i^{\alpha}}{2}\left[5k\left(T^{\beta} - T^{\alpha}\right) + m^{\beta}\left|\boldsymbol{v}^{\beta} - \boldsymbol{v}^{\alpha}\right|^2\right]\right\},
\end{aligned} \tag{13b}$$

with $c_i^{\alpha} = \xi_i - v_i^{\alpha}$. Here $\overline{A_{ij}}$ denotes the symmetrized traceless part of a square matrix A_{ij} of order three and is defined as

$$\overline{A_{ij}} = \frac{1}{2}\left(A_{ij} + A_{ji} - \frac{2}{3}A_{kk}\delta_{ij}\right), \tag{14}$$

where δ_{ij} is the Kronecker delta. The $\eta^{\beta\alpha}$ is a constant defined as

$$\eta^{\beta\alpha} = 2\pi\left(a^{\beta\alpha}/\mu^{\beta\alpha}\right)^{1/2} B\left(g_c^{\beta\alpha}\right), \qquad B(z) = 6\int_0^z g\sin^2\theta\cos^2\theta\,\mathrm{d}g. \tag{15}$$

Finally, we would like to comment about the case of the Maxwell molecule, that is, the case where the angular cutoff is not introduced. Since $g(\pi/2) = \infty$ [see the sentence after Eq. (7)], $K^{\beta\alpha}$ in Eq. (9) diverges. In contrast, the coefficients $\chi^{\beta\alpha}$ and $\eta^{\beta\alpha}$

remain finite even without the angular cutoff, since $A(\infty) = 0.597$ and $B(\infty) = 0.925$.

3. Model equations for gas mixtures

In this section, we shall first show two existing model equations and then introduce the polynomial model newly constructed in the present contribution. Those three models will later be compared numerically with the Boltzmann equation. The following notation will be used:

$$M(\boldsymbol{\xi}; \boldsymbol{a}, A_{ij}) = \frac{1}{(2\pi)^{3/2}|A_{ij}|^{1/2}} \exp\left(-\frac{1}{2} {A_{ij}}^{-1}(\xi_i - a_i)(\xi_j - a_j)\right). \tag{16}$$

Here A_{ij} is a square matrix of order three and $|A_{ij}|$ is its determinant.

3.1. Existing models

3.1.1. Andries, Aoki, and Perthame's model

The model equation proposed by Andries, Aoki, and Perthame [18] may be written as Eq. (1) with $J^{\beta\alpha}$ being replaced by the following model collision term $J_M^{\beta\alpha}$:

$$J_M^{\beta\alpha} = K_M^{\beta\alpha} n^\beta \left(n^\alpha M\left(\boldsymbol{\xi}; \boldsymbol{v}^{(\alpha)}, \frac{kT^{(\alpha)}}{m^\alpha}\delta_{ij}\right) - f^\alpha\right). \tag{17}$$

Here $K_M^{\beta\alpha}$ $(= K_M^{\alpha\beta})$ is a positive constant. The $\boldsymbol{v}^{(\alpha)}$ and $T^{(\alpha)}$ are defined as

$$\boldsymbol{v}^{(\alpha)} = \boldsymbol{v}^\alpha + \frac{2}{K_M^\alpha} \sum_\gamma \frac{\chi_M^{\gamma\alpha} m^\gamma n^\gamma}{m^\gamma + m^\alpha} (\boldsymbol{v}^\gamma - \boldsymbol{v}^\alpha), \tag{18a}$$

$$T^{(\alpha)} = T^\alpha - \frac{m^\alpha}{3k}|\boldsymbol{v}^{(\alpha)} - \boldsymbol{v}^\alpha|^2 + \frac{2}{K_M^\alpha} \sum_\gamma \frac{\chi_M^{\gamma\alpha} \mu^{\gamma\alpha} n^\gamma}{m^\gamma + m^\alpha} \left(T^\gamma - T^\alpha + \frac{m^\gamma}{3k}|\boldsymbol{v}^\gamma - \boldsymbol{v}^\alpha|^2\right), \tag{18b}$$

where $K_M^\alpha = \sum_\gamma K_M^{\gamma\alpha} n^\gamma$ and $\chi_M^{\beta\alpha}$ $(= \chi_M^{\alpha\beta})$ is another positive constant. The inequality $0 < \chi_M^{\beta\alpha} \leqslant K_M^{\beta\alpha}$ must be hold in order to keep $T^{(\alpha)}$ positive.

The collision frequency $\nu^{\beta\alpha}$ for this model is given by Eq. (9a) with $K^{\beta\alpha}$ being replaced by the constant $K_M^{\beta\alpha}$. In addition, the moments of $J_M^{\beta\alpha}$ with respect to $m^\alpha \xi_i$ and $m^\alpha |\boldsymbol{\xi}|^2/2$ are given by Eqs. (11a) and (11b) with $\chi^{\beta\alpha}$ being replaced by $\chi_M^{\beta\alpha}$. This means that if one sets $K_M^{\beta\alpha} = K^{\beta\alpha}$ and $\chi_M^{\beta\alpha} = \chi^{\beta\alpha}$ with $K^{\beta\alpha}$ and $\chi^{\beta\alpha}$ being calculated from Eqs. (9b) and (12), the collision frequency and collisional transfer of momentum and that of energy for this model coincide with those for the Boltzmann equation for the pseudo Maxwell molecules. In this sense, one can say that the Andries, Aoki, and Perthame's model is a model equation for the pseudo Maxwell molecular gases.

Higher-order moments of $J_M^{\beta\alpha}$ (with respect to $m^\alpha \overline{c_i^\alpha c_j^\alpha}$ and $m^\alpha c_i^\alpha |\boldsymbol{c}^\alpha|^2/2$), however, do not have the same forms as Eqs. (13a) and (13b). Therefore, those moments cannot be matched to their counterparts of the Boltzmann equation in general. Finally it should be noted that this model is proved to satisfy the H-theorem (see Ref. [18]).

3.1.2. ES-BGK model for mixtures

The ES-BGK model for mixtures proposed by Holway [4,5] may be written as Eq. (1) with $J^{\beta\alpha}$ being replaced by the following $J_M^{\beta\alpha}$:

$$J_M^{\beta\alpha} = K_M^{\beta\alpha} n^\beta \left(n^\alpha M(\boldsymbol{\xi}; \boldsymbol{v}^{\beta\alpha}, \tau_{ij}^{\beta\alpha}) - f^\alpha\right). \tag{19}$$

Here $K_M^{\beta\alpha}$ $(= K_M^{\alpha\beta})$ is a positive constant. The $\boldsymbol{v}^{\beta\alpha}$ and $\tau_{ij}^{\beta\alpha}$ are defined as

$$\boldsymbol{v}^{\beta\alpha} = \boldsymbol{v}^\alpha + \frac{\chi_M^{\beta\alpha}}{K_M^{\beta\alpha}} \frac{\mu^{\beta\alpha}}{m^\alpha} (\boldsymbol{v}^\beta - \boldsymbol{v}^\alpha), \tag{20a}$$

$$\tau_{ij}^{\beta\alpha} = \frac{p_{ij}^\alpha}{\rho^\alpha} + \frac{\chi_M^{\beta\alpha}}{K_M^{\beta\alpha}} \left(\frac{\mu^{\beta\alpha}}{m^\alpha}\right)^2 \times \left[\frac{p_{ij}^\beta}{\rho^\beta} - \frac{m^\alpha}{m^\beta}\frac{p_{ij}^\alpha}{\rho^\alpha} + \left(1 - \frac{\chi_M^{\beta\alpha}}{K_M^{\beta\alpha}}\right)(v_i^\beta - v_i^\alpha)(v_j^\beta - v_j^\alpha)\right] - \frac{\eta_M^{\beta\alpha}}{2K_M^{\beta\alpha}} \left(\frac{\mu^{\beta\alpha}}{m^\alpha}\right)^2 \left[\frac{\overline{p_{ij}^\beta}}{\rho^\beta} + \frac{\overline{p_{ij}^\alpha}}{\rho^\alpha} + \overline{(v_i^\beta - v_i^\alpha)(v_j^\beta - v_j^\alpha)}\right], \tag{20b}$$

where $\chi_M^{\beta\alpha}$ $(= \chi_M^{\alpha\beta})$ and $\eta_M^{\beta\alpha}$ $(= \eta_M^{\alpha\beta})$ are positive constants. These constants must satisfy the following conditions in order to keep $\tau_{ij}^{\beta\alpha}$ positive definite: $0 < \eta_M^{\alpha\alpha} \leqslant (3/2)K_M^{\alpha\alpha}$ and $0 < \chi_M^{\beta\alpha} \leqslant K_M^{\beta\alpha}$ and $0 < \eta_M^{\beta\alpha} \leqslant 3\chi_M^{\beta\alpha}(1 - \chi_M^{\beta\alpha}/K_M^{\beta\alpha})$ for $\beta \neq \alpha$.

As in the case of the Andries et al.'s model, the collision frequency and collisional transfer of momentum and that of energy for the ES-BGK model are, respectively, given by Eq. (9a) with $K^{\beta\alpha}$ being replaced by $K_M^{\beta\alpha}$ and Eqs. (11a) and (11b) with $\chi^{\beta\alpha}$ being replaced by $\chi_M^{\beta\alpha}$. Furthermore, the moment of $J_M^{\beta\alpha}$ with respect to $m^\alpha \overline{c_i^\alpha c_j^\alpha}$ is given by Eq. (13a) with $\chi^{\beta\alpha}$ and $\eta^{\beta\alpha}$ being replaced by $\chi_M^{\beta\alpha}$ and $\eta_M^{\beta\alpha}$ respectively. However the moment with respect to $m^\alpha c_i^\alpha |\boldsymbol{c}^\alpha|^2/2$ does not have the same form as Eq. (13b) (see Ref. [27]).

The ES-BGK model is suitable for the pseudo Maxwell molecular gases for the same reason as that in the case of the Andries et al.'s model. Since an additional moment of the collision term (with respect to $m^\alpha \overline{c_i^\alpha c_j^\alpha}$) can be matched to its counterpart of the original Boltzmann equation, one may expect that the ES-BGK model equation gives results closer to those of the original one than the Andries et al.'s model does. As will be seen later in the numerical examples in Section 4, this expectation is true in some sense. However, although the ES-BGK model for a single-component gas satisfies the H-theorem as proven in Ref. [6], the corresponding proof in the case of mixtures has not yet been known.

3.2. New polynomial model

We shall show below the polynomial model for gas mixtures, which we derived by following essentially the same procedure as that employed in the construction of the McCormack model [20] in the linearized kinetic theory. We first write the model collision term $J_M^{\beta\alpha}$ in the following form:

$$J_M^{\beta\alpha} = M\left(\boldsymbol{\xi}; \boldsymbol{v}, \frac{kT}{m^\alpha}\delta_{ij}\right) \Phi^{\beta\alpha} - K_M^{\beta\alpha} n^\beta f^\alpha. \tag{21}$$

Here $K_M^{\beta\alpha}$ $(= K_M^{\alpha\beta})$ is a positive constant and $\Phi^{\beta\alpha}$ is a polynomial in ξ_i given by

$$\Phi^{\beta\alpha} = K_M^{\beta\alpha} n^\beta n^\alpha + 2\zeta_i^\alpha \Phi_{(1)i}^{\beta\alpha} + \left(|\boldsymbol{\zeta}^\alpha|^2 - \frac{3}{2}\right)\Phi_{(2)}^{\beta\alpha} + \zeta_i^\alpha \zeta_j^\alpha \Phi_{(3)ij}^{\beta\alpha} + \frac{4}{5}\zeta_i^\alpha \left(|\boldsymbol{\zeta}^\alpha|^2 - \frac{5}{2}\right)\Phi_{(4)i}^{\beta\alpha}, \tag{22a}$$

$$\boldsymbol{\zeta}^\alpha = \sqrt{\frac{m^\alpha}{2kT}}(\boldsymbol{\xi} - \boldsymbol{v}). \tag{22b}$$

The $\Phi_{(1)i}^{\beta\alpha}$, $\Phi_{(2)}^{\beta\alpha}$, $\Phi_{(3)ij}^{\beta\alpha}$, and $\Phi_{(4)i}^{\beta\alpha}$ in Eq. (22a) are constants with respect to $\boldsymbol{\xi}$ (or $\boldsymbol{\zeta}^\alpha$), and are determined so that the model collision term $J_M^{\beta\alpha}$ in Eq. (21) and the original collision term $J^{\beta\alpha}$ in

Eq. (2a) for Grad's 13-moment approximation [28,23] to the velocity distribution function yield the same moments. More precisely, $\Phi^{\beta\alpha}_{(1)i}$, $\Phi^{\beta\alpha}_{(2)}$, etc. are determined so that the following relation is satisfied:

$$\int h(\boldsymbol{\xi}) J^{\beta\alpha}\left(f^{\beta}_{M}, f^{\alpha}_{M}\right) \mathrm{d}^3\xi = \int h(\boldsymbol{\xi}) J^{\beta\alpha}_{M} \,\mathrm{d}^3\xi, \quad \text{for } h(\boldsymbol{\xi}) = 1, \boldsymbol{\xi}, \xi_i\xi_j, \xi_i|\boldsymbol{\xi}|^2. \tag{23}$$

Here f^{α}_{M} is Grad's 13-moment approximation to the velocity distribution function, which is written as

$$f^{\alpha}_{M} = M\left(\boldsymbol{\xi}; \boldsymbol{v}, \frac{kT}{m^{\alpha}}\delta_{ij}\right)\left[n^{\alpha} + 2\zeta^{\alpha}_{k}A^{\alpha}_{k} + \left(|\boldsymbol{\zeta}^{\alpha}|^2 - \frac{3}{2}\right)B^{\alpha} + \zeta^{\alpha}_{k}\zeta^{\alpha}_{l}C^{\alpha}_{kl} + \frac{4}{5}\zeta^{\alpha}_{k}\left(|\boldsymbol{\zeta}^{\alpha}|^2 - \frac{5}{2}\right)D^{\alpha}_{k}\right], \tag{24}$$

with

$$A^{\alpha}_{i} = \sqrt{\frac{m^{\alpha}}{2kT}}n^{\alpha}\left(v^{\alpha}_{i} - v_i\right), \qquad B^{\alpha} = \frac{n^{\alpha}}{T}\left(T^{\alpha} - T + \frac{m^{\alpha}}{3k}|\boldsymbol{v}^{\alpha} - \boldsymbol{v}|^2\right),$$
$$C^{\alpha}_{ij} = \frac{1}{kT}\left[\overline{p^{\alpha}_{ij}} + m^{\alpha}n^{\alpha}\overline{\left(v^{\alpha}_{i} - v_i\right)\left(v^{\alpha}_{j} - v_j\right)}\right],$$
$$D^{\alpha}_{i} = \frac{1}{kT}\sqrt{\frac{m^{\alpha}}{2kT}}\left\{q^{\alpha}_{i} + \overline{p^{\alpha}_{ij}}\left(v^{\alpha}_{j} - v_j\right) + \frac{v^{\alpha}_{i} - v_i}{2}\left[5kn^{\alpha}\left(T^{\alpha} - T\right) + \rho^{\alpha}|\boldsymbol{v}^{\alpha} - \boldsymbol{v}|^2\right]\right\}. \tag{25}$$

The expressions of $\Phi^{\beta\alpha}_{(1)i}$, $\Phi^{\beta\alpha}_{(2)}$, etc. determined by Eq. (23) are tremendously complicated and are shown only in Eqs. (A.1a)–(A.1d) in Appendix A. They are written in terms of the macroscopic quantities and Chapman–Cowling's Ω integrals [23]. The latter depends on the molecular model and can be defined in terms of the function $B^{\beta\alpha}$ as shown in Eq. (A.4) in Appendix A. Specific forms of the Ω integrals for the HS and pseudo Maxwell molecule are shown in Eqs. (A.5) and (A.6).

Since A^{α}_{i}, B^{α}, C^{α}_{ij}, and D^{α}_{i} in Eq. (25) vanish (or $v^{\alpha}_{i} = v_i$, $T^{\alpha} = T$, $\overline{p^{\alpha}_{ij}} = 0$, and $q^{\alpha}_{i} = 0$) in an equilibrium state, they are usually expected to be small in many cases. In the expressions of $\Phi^{\beta\alpha}_{(1)i}$, $\Phi^{\beta\alpha}_{(2)}$, etc. in Eqs. (A.1a)–(A.1d), however, all the cross terms (second order terms with respect to A^{α}_{i}, B^{α}, C^{α}_{ij}, and D^{α}_{i}) are retained. We should note that some of the cross terms may become negligibly small [or smaller than terms which have already been omitted in Eq. (24)] depending on the situation. If one considers the case of the linear problem, that is, the case where the state of the mixture deviates only slightly from a uniform equilibrium state at rest, and linearizes the above polynomial model in the standard manner, one obtains the third-order McCormack model. Moreover, if one considers the case of a single-component gas and omits the second order terms with respect to C^{α}_{ij} and D^{α}_{i} (those terms automatically vanish in the case of the Maxwell molecule; see the last sentence in Appendix A), the polynomial model reduces to Liu's model [29]. Similar type of model for the nonlinear Boltzmann equation, which uses a polynomial in the expression of the collision term, has been proposed also in Refs. [30–33] in the case of a single-component gas, and in Refs. [12,17] in the case of a mixture.[1]

Unlike Andries et al.'s and ES-BGK models, the polynomial model introduced here is not restricted to the pseudo Maxwell molecule but can fit to various molecular models by the use of the Ω integrals for specific molecular models. However, one should note that the collision frequency for the polynomial model is given by Eq. (9a) with $K^{\beta\alpha}$ being replaced by $K^{\beta\alpha}_{M}$ and does not depend on the molecular velocity $\boldsymbol{\xi}$. This is true for the Boltzmann equation only when a peculiar molecular model, such as the pseudo Maxwell molecule, whose function $B^{\beta\alpha}$ is independent of $|\boldsymbol{V}|$ is employed [see Eqs. (8) and (6)]. The transport coefficients obtained by applying the Chapman–Enskog method [23] to the polynomial model coincide with those counterparts of the McCormack model and also with those of the original Boltzmann equation at the first or second approximation. More precisely, the viscosity, thermal conductivity, and thermal diffusion coefficient coincide at the first approximation, and the diffusion coefficient up to the second approximation. See Ref. [34] for details of the multicomponent transport coefficients and for the nomenclature of the first or second approximation. Their expressions in the case of binary mixtures are given in Refs. [35,36] for general molecular models and Appendix B for the pseudo Maxwell molecule. As for the H-theorem, the proof similar to that in Ref. [29] for the Liu's model is possible, provided that the distribution f^{α} is very close to the local equilibrium. This is consistent with the fact that the polynomial model reduces to the McCormack model, which satisfies the H-theorem, after the linearization around an equilibrium state.

In the case of the pseudo Maxwell molecules, moments of $J^{\beta\alpha}_{M}$ with respect to $m^{\alpha}\xi_i$, $m^{\alpha}|\boldsymbol{\xi}|^2/2$, $m^{\alpha}\overline{c^{\alpha}_{i}c^{\alpha}_{j}}$, and $m^{\alpha}c^{\alpha}_{i}|\boldsymbol{c}^{\alpha}|^2/2$ completely coincide with corresponding results of the Boltzmann equation, that is, Eqs. (11) and (13). Consequently, as will be seen later in the numerical examples in Section 4, the above model reproduces results of the Boltzmann equation better than the Andries et al.'s and ES-BGK model do, unless the mixture is in a strong nonequilibrium.

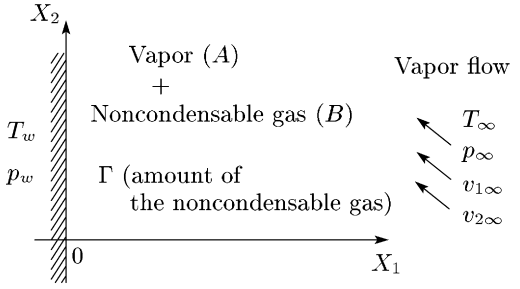

Fig. 1. Problem.

4. Numerical comparisons

In this section, we first make a numerical comparison between the Boltzmann equation for the pseudo Maxwell molecules and the three model equations introduced in the previous section. Then we make a numerical comparison between the Boltzmann equation for the hard-sphere (HS) molecules and the polynomial model introduced in Section 3.2 only, since the other two models are not suitable for the HS molecular gases. The former comparison is performed in a half-space problem of a vapor condensing onto a plane condensed phase in the presence of a noncondensable gas. The latter is performed not only in the same half-space problem but also in the two-surface problem of a vapor–gas mixture.

4.1. Case of the pseudo Maxwell molecules

4.1.1. Description of the problem

The comparison in the case of the pseudo Maxwell molecule is performed in the problem shown in Fig. 1. Let us consider a binary mixture of a vapor (species A) of a condensed phase and a noncondensable gas (species B) in a half space ($X_1 > 0$).

[1] In the case of the Maxwell molecule, the polynomial model derived here reduces to the extended version of Garzó, Santos, and Brey's model [17] which we introduced previously in Ref. [19], if one sets $C^{\alpha}_{ij} = D^{\alpha}_{i} = 0$ and $\Phi^{\beta\alpha}_{(3)ij} = \Phi^{\beta\alpha}_{(4)i} = 0$ (5-moment approximation).

The condensed phase is located at $X_1 = 0$ and kept at temperature T_w. The p_w is the saturation pressure of the vapor at temperature T_w. From the infinity ($X_1 \to \infty$), the pure vapor at the equilibrium state with pressure p_∞, temperature T_∞, and velocity $\boldsymbol{v}_\infty$ [$= (v_{1\infty}, v_{2\infty}, 0)$; $v_{1\infty} < 0, v_{2\infty} \geqslant 0$] is flowing, and a steady condensation is taking place at the surface of the condensed phase. Then we investigate the steady behavior of the mixture. The boundary condition at $X_1 = 0$ is the complete condensation for the vapor[2] and the diffuse reflection for the noncondensable gas. The parameter Γ appearing in Fig. 1 indicates the total amount of the noncondensable gas in the half space, which is defined as

$$\Gamma = \frac{2}{\sqrt{\pi}} \frac{1}{n_\infty \ell_\infty} \int_0^\infty n^B \, \mathrm{d}X_1, \quad n_\infty = \frac{p_\infty}{kT_\infty}. \tag{26}$$

Here ℓ_∞ [$\equiv (8kT_\infty/\pi m^A)^{1/2}/K^{AA} n_\infty$] is the mean free path of a vapor molecule in the equilibrium state at rest with number density n_∞ and temperature T_∞.

The comprehensive analysis of this problem, in the case where molecules of the vapor and noncondensable gas are mechanically identical, has already been performed in Refs. [37–40] on the basis of Garzó, Santos, and Brey's model equation [17]. As a result, the relation between the parameters appearing in Fig. 1 for solutions to exist is established. In the case of the subsonic condensation ($M_{n\infty} < 1$), the relation is written as

$$\begin{aligned} &p_\infty/p_w = \mathcal{F}_s(M_{n\infty}, M_{t\infty}, T_\infty/T_w, \Gamma), \\ &0 \leqslant \Gamma \leqslant \Gamma_*(M_{n\infty}, M_{t\infty}, T_\infty/T_w), \end{aligned} \tag{27}$$

where $M_{n\infty}$ ($\equiv -v_{1\infty}/a_\infty$) and $M_{t\infty}$ ($\equiv v_{2\infty}/a_\infty$) are the Mach number of the normal and tangential flow at infinity and a_∞ [$\equiv (5kT_\infty/3m^A)^{1/2}$] is the sound speed in the pure vapor at temperature T_∞. The $\mathcal{F}_s$ and Γ_* are functions of the arguments indicated in Eq. (27): their numerical data are tabulated in Refs. [37–39].[3] The second equation of Eq. (27) means that Γ_* is the maximum amount of the noncondensable gas that can exist in the half space for particular values of $M_{n\infty}$, $M_{t\infty}$, and T_∞/T_w. See Refs. [37,38,40] for the corresponding relation in the case of the supersonic condensation ($M_{n\infty} \geqslant 1$).

The dimensionless parameters characterizing the problem in the case of the Boltzmann equation for the pseudo Maxwell molecules are the following: T_∞/T_w, p_∞/p_w, $M_{n\infty}$, $M_{t\infty}$, m^B/m^A, a^{BB}/a^{AA}, a^{BA}/a^{AA}, g_c^{AA}, g_c^{BB}, g_c^{BA}, and Γ. Here we limit ourselves to the case of $T_\infty/T_w = 1$, $a^{BB}/a^{AA} = a^{BA}/a^{AA} = 1$, and $g_c^{AA} = g_c^{BB} = g_c^{BA}$ ($\equiv g_c$), and perform computations for several values of $M_{n\infty}$ (< 1), $M_{t\infty}$, m^B/m^A, g_c, and Γ ($\leqslant \Gamma_*$). Then the value of p_∞/p_w will be determined simultaneously with the solution so that Eq. (27) is satisfied. In order to make proper comparisons between the Boltzmann and model equations, parameters appearing in the models are determined so that the collision frequency and moments of the collision term coincide. That is, we set $(K_M^{\beta\alpha}, \chi_M^{\beta\alpha}) = (K^{\beta\alpha}, \chi^{\beta\alpha})$ for the Andries et al.'s model and $(K_M^{\beta\alpha}, \chi_M^{\beta\alpha}, \eta_M^{\beta\alpha}) = (K^{\beta\alpha}, \chi^{\beta\alpha}, \eta^{\beta\alpha})$ for the ES-BGK model, where $K^{\beta\alpha}$, $\chi^{\beta\alpha}$, and $\eta^{\beta\alpha}$ are calculated from Eqs. (9b), (12), and (15) for the pseudo Maxwell molecule. In the case of the polynomial model, we set $K_M^{\beta\alpha} = K^{\beta\alpha}$ and use Chapman–Cowling's Ω integrals for the pseudo Maxwell molecule shown in Eq. (A.6) in Appendix A. Since the inequality $0 < \chi^{\beta\alpha} \leqslant K^{\beta\alpha}$ is easily derived from Eqs. (9b) and (12), one can see that $T^{(\alpha)}$ appearing in the Andries et al.'s model is always positive in the above parameter setting [see the sentence after Eq. (18)]. The positive definiteness of $\tau_{ij}^{\beta\alpha}$ appearing in the ES-BGK model will be checked later. The Boltzmann equation is solved by means of the direct simulation Monte Carlo (DSMC) method [1], and the model equations are by means of a finite-difference method.

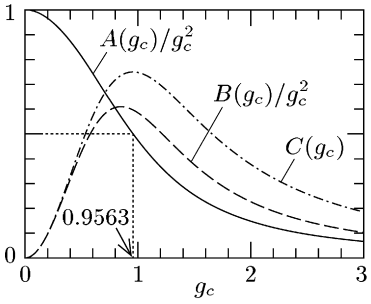

Fig. 2. $A(g_c)/g_c^2$, $B(g_c)/g_c^2$, and $C(g_c)$ vs. g_c.

The problem described above is the same problem as that considered previously in Ref. [19] and may seem to be rather special. We think, however, that it is a good sample problem to illustrate some nature of model equations for mixtures. Since the species B is a noncondensable gas, it cannot penetrate into the condensed phase and its flow velocity along the X_1-axis is identically zero ($v_1^B \equiv 0$). Therefore one can adjust freely the strength of the diffusion (i.e., $|v_1^A - v_1^B|$) by changing the normal Mach number at infinity $M_{n\infty}$. In addition, one can inspect the effect of the shear by putting a tangential flow at infinity, i.e., nonzero $M_{t\infty}$.

4.1.2. Results and discussions

As mentioned in the previous section, $T^{(\alpha)}$ appearing in the Andries et al.'s model is always positive in our parameter setting, since $0 < \chi^{\beta\alpha} \leqslant K^{\beta\alpha}$. Let us first check the positive definiteness of $\tau_{ij}^{\beta\alpha}$ appearing in the ES-BGK model [see the sentence after Eq. (20)]. It can be easily seen that the inequality $0 < \eta^{\alpha\alpha} \leqslant (3/2)K^{\alpha\alpha}$ follows from Eqs. (9b) and (15). In Fig. 2, $A(g_c)/g_c^2$ ($= \chi^{\beta\alpha}/K^{\beta\alpha}$), $B(g_c)/g_c^2$ ($= \eta^{\beta\alpha}/K^{\beta\alpha}$), and $C(g_c)$ [$\equiv 3(\chi^{\beta\alpha}/K^{\beta\alpha})(1 - \chi^{\beta\alpha}/K^{\beta\alpha})$] are shown as functions of g_c [see Eqs. (9b), (12), and (15)]. Fig. 2 indicates that the inequality $B(g_c)/g_c^2 \leqslant C(g_c)$ holds in a wide range of g_c, which means that $\tau_{ij}^{\beta\alpha}$ is positive definite in a wide range of g_c in our parameter setting.

Figs. 3–5 show profiles of the macroscopic quantities in the case of a relatively weak condensation ($M_{n\infty} = 0.1$): Figs. 3 and 4 are for $m^B/m^A = 1$ (i.e., molecules are mechanically identical) and Fig. 5 for $m^B/m^A = 5$. In those figures, results for the cutoff parameter $g_c = 0.9563$ (the corresponding cutoff angle is $\theta_c = 63.15°$)[4] and for $g_c = 2$ ($\theta_c = 86.27°$) are shown. The results of the Boltzmann equation and Andries et al.'s model in the figures were obtained in our previous work [19] and are shown again to make comparison with results of the ES-BGK and polynomial models obtained in the present work. Here the space coor-

[2] The vapor molecules leaving the condensed phase are distributed according to the Maxwell distribution with temperature T_w and the saturation pressure p_w. See, e.g., Ref. [25].

[3] In general, $\mathcal{F}_s$ and Γ_* in Eq. (27) depend also on the parameters concerning the molecules (i.e., the molecular mass m^α and so on) and also on the equation. Therefore, the tabulated data of them in Refs. [37–39], which are obtained by Garzó, Santos, and Brey's model in the case of the mechanically identical molecules, cannot be used directly in the present analyses based on the Boltzmann equation and models in Section 3.

[4] As seen in Fig. 2, $\chi^{\beta\alpha}/K^{\beta\alpha}$ [$= A(g_c)/g_c^2] = 1/2$ at $g_c = 0.9563$. Incidentally, in the case of the model equation proposed by Hamel [14] and that by Garzó, Santos, and Brey [17], the coefficient $K^{\beta\alpha}$ and $\chi^{\beta\alpha}$ are not independent and satisfy $\chi^{\beta\alpha}/K^{\beta\alpha} = 1/2$. Since the Andries et al.'s model yields results very close to those of the Hamel's and Garzó et al.'s model in the case of a weak condensation (see Ref. [19]), results of the former model for $g_c = 0.9563$ in Figs. 3(a), 4(a), and 5(a) are almost the same as those of the latter two models.

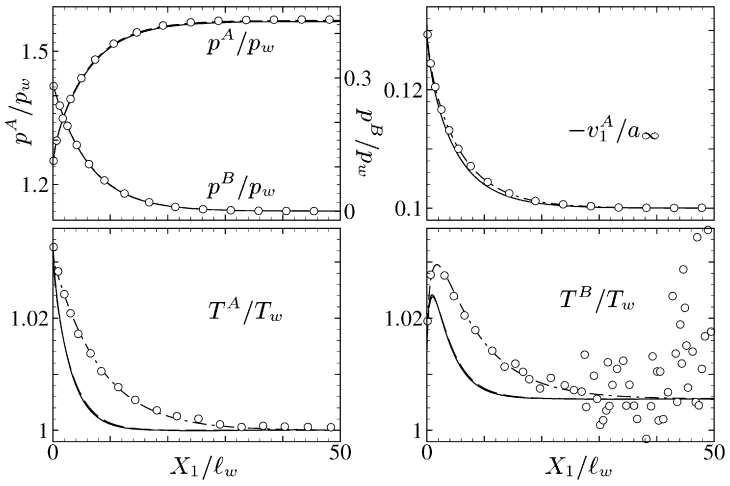

(a) $g_c = 0.9563$

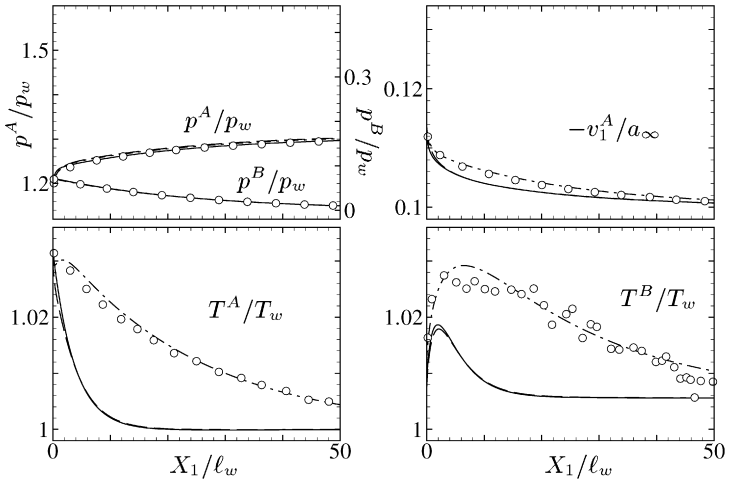

(b) $g_c = 2$

Fig. 3. Profiles of the macroscopic quantities for $M_{n\infty} = 0.1$, $M_{t\infty} = 0$, $m^B/m^A = 1$, and $\Gamma = 2$. (a) $g_c = 0.9563$ ($\theta_c = 63.15°$) and (b) $g_c = 2$ ($\theta_c = 86.27°$). The —— indicates results of the Andries et al.'s model, – – – those of the ES-BGK model, – · – those of the polynomial model, and ∘ those of the Boltzmann equation for the pseudo Maxwell molecules.

dinate X_1 is normalized by the reference mean free path $\ell_w = (8kT_w/\pi m^A)^{1/2}/K^{AA}n_w$ with $n_w = p_w/kT_w$. The profiles of T^B and v_2^B for the Boltzmann equation obtained by the DSMC method fluctuate at the far field from the condensed phase, since p^B is vanishing there and so the number of simulation particles for species B is very small.

The slope of profiles obtained by the Boltzmann equation becomes gradual at $g_c = 2$ compared with that at $g_c = 0.9563$. All the models give almost the same profiles of p^α ($\alpha = A, B$), which almost coincide with those by the Boltzmann equation, irrespective of the value of g_c. However, profiles of v_2^α and T^α obtained by the Andries et al.'s model differ significantly from those by the Boltzmann equation and depend only weakly on g_c. The profiles of v_2^α obtained by the ES-BGK model and those by the polynomial model agree well and almost coincide with those by the Boltzmann equation. As for the profiles of T^α, only the results by the polynomial model show good agreement with those by the Boltzmann equation.

As clarified in Ref. [41], the flow field for $M_{n\infty} \to 0$ can be described by the fluid-dynamic equations (see also Refs. [42–44]).[5]

The behavior of the macroscopic quantities in Figs. 3–5 may, therefore, be explained by the dependence on g_c of the transport coefficients, i.e., the viscosity μ, thermal conductivity λ, and mutual diffusion coefficient D_{AB}. Their first approximations in the Chapman–Enskog method are shown in Appendix B. In the present parameter setting, the Andries et al.'s model reproduces a correct value of D_{AB}, while μ and λ do not coincide with those of the Boltzmann equation. In the case of the ES-BGK model, μ as well as D_{AB} is correct, while λ is not. In the case of the polynomial model, λ in addition to D_{AB} and μ is also correct. Let us write $D_{AB} = (kT/nm^AK^{AA})\hat{D}_{AB}$, $\mu = (kT/K^{AA})\hat{\mu}$, and $\lambda = (5k^2T/2m^AK^{AA})\hat{\lambda}$, and consider the simple case of mechanically identical molecules (the case of Figs. 3 and 4). Then we have $\hat{D}_{AB} = g_c^2/A(g_c)$ and $\hat{\mu} = (2/3)\hat{\lambda} = g_c^2/B(g_c)$ for the Boltzmann equation and the polynomial model, which mean that $\hat{D}_{AB}$ increases monotonically with increasing g_c and $\hat{\mu}$ and $\hat{\lambda}$ have their minimum at $g_c \sim 0.8$ (see Fig. 2). On the other hand, the Andries et al.'s model gives the correct $\hat{D}_{AB}$ but $\hat{\mu} = \hat{\lambda} = 1$, i.e., $\hat{\mu}$ and $\hat{\lambda}$ independent of g_c. In the case of the ES-BGK model, $\hat{D}_{AB}$ and $\hat{\mu}$ are correct, but $\hat{\lambda} = 1$.

We performed computations also in the case of relatively strong condensations ($M_{n\infty} = 0.5$ and 0.9), but omit their results because the macroscopic quantities obtained by the polynomial model show unphysical behavior for $M_{n\infty} \gtrsim 0.5$. The polynomial model reproduces correct behavior of the macroscopic quantities

[5] Note that the length scale of variations of the macroscopic quantities in Figs. 3–5 for $M_{n\infty} = 0.1$ (the case of a relatively weak condensation) is much larger than the mean free path.

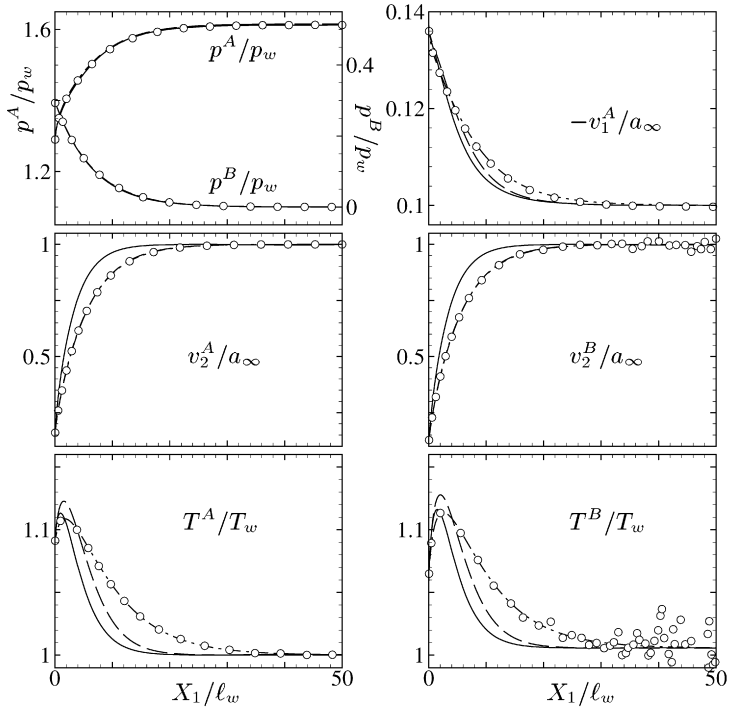

(a) $g_c = 0.9563$

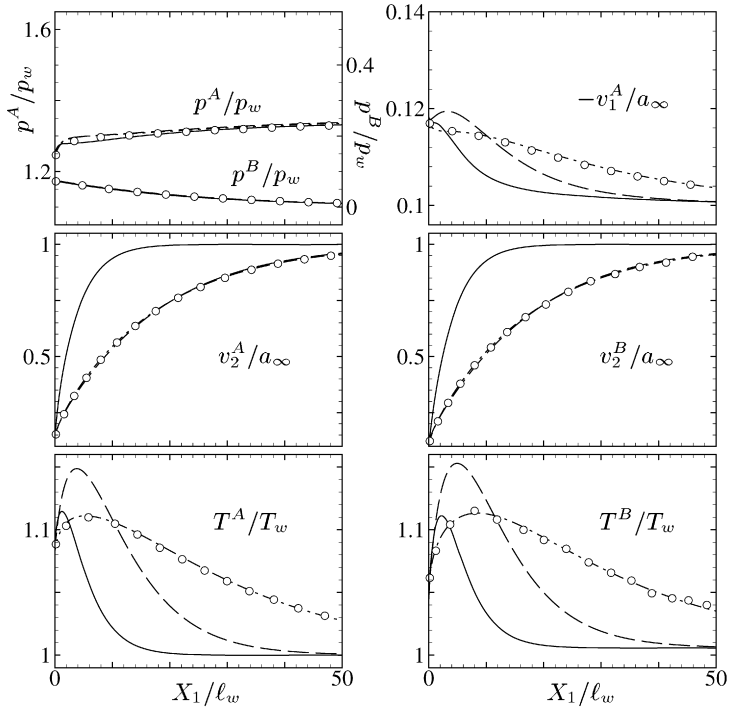

(b) $g_c = 2$

Fig. 4. Profiles of the macroscopic quantities for $M_{n\infty} = 0.1$, $M_{t\infty} = 1$, $m^B/m^A = 1$, and $\Gamma = 2$. (a) $g_c = 0.9563$ ($\theta_c = 63.15°$) and (b) $g_c = 2$ ($\theta_c = 86.27°$). See the caption of Fig. 3.

in Figs. 3–5 (in the case of a relatively weak condensation), while slightly negative values of the velocity distribution function are observed. In general, this phenomenon could happen when one constructs models of the collision term by the use of polynomials as we did in Section 3.2. The $\Phi^{\beta\alpha}_{(1)i}$, $\Phi^{\beta\alpha}_{(2)}$, etc. in Eq. (22a) vanish at an equilibrium state but their absolute values generally increase as the state deviates from the equilibrium [see Eq. (A.1) in Appendix A]. Since $M_{n\infty}$ gives a measure of the nonequilibrium in the present problem, $|\Phi^{\beta\alpha}_{(1)i}|$, $|\Phi^{\beta\alpha}_{(2)}|$, etc. increase with increasing $M_{n\infty}$, which could cause the remarkably negative value of $\Phi^{\beta\alpha}$ in Eq. (22a). As a result, when the condensation becomes strong ($M_{n\infty} \gtrsim 0.5$), unphysical behavior will be observed also at the level of the macroscopic quantities. Previously in Ref. [19], we performed computations for the same half-space problem using the Garzó et al.'s model, which also uses a polynomial in the expression of the collision term, while no unphysical behavior of the

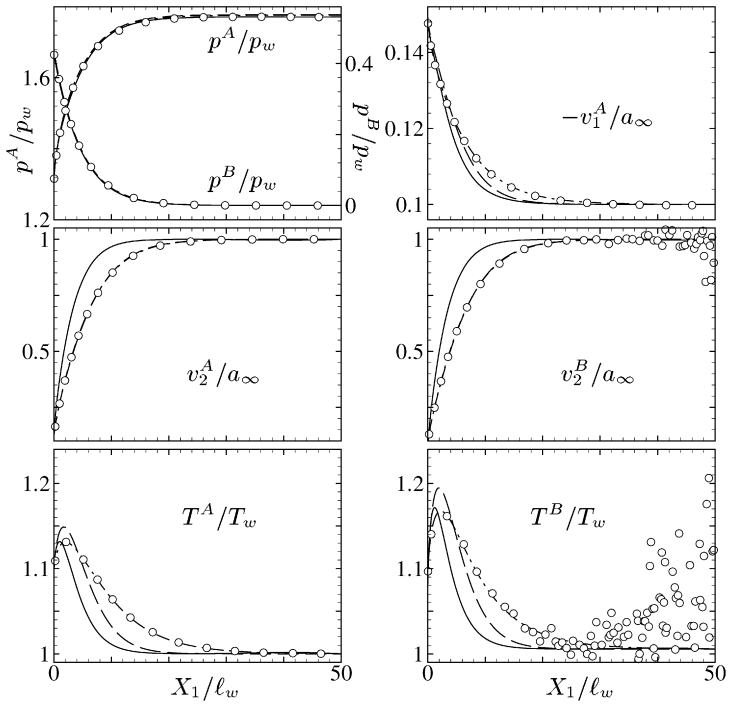

(a) $g_c = 0.9563$

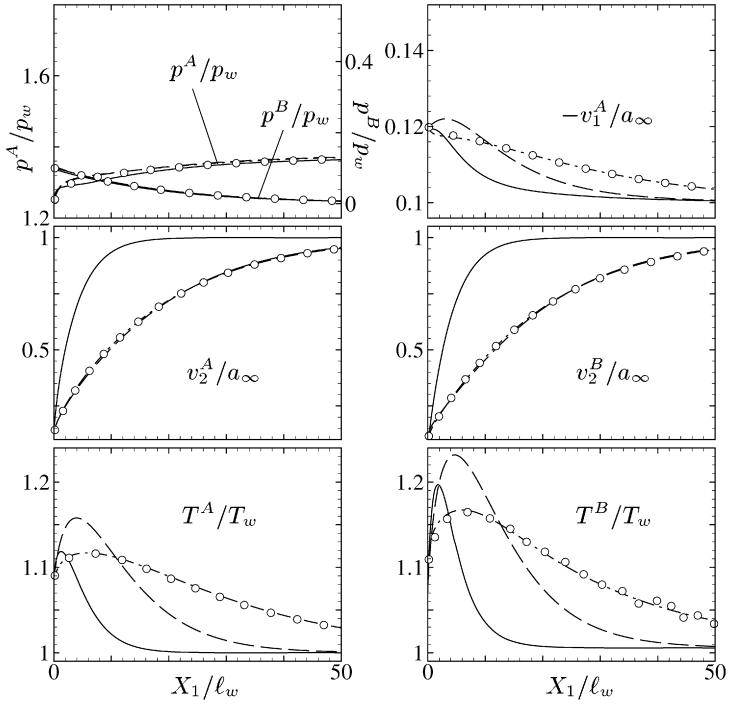

(b) $g_c = 2$

Fig. 5. Profiles of the macroscopic quantities for $M_{n\infty} = 0.1$, $M_{t\infty} = 1$, $m^B/m^A = 5$, and $\Gamma = 2$. (a) $g_c = 0.9563$ ($\theta_c = 63.15°$) and (b) $g_c = 2$ ($\theta_c = 86.27°$). See the caption of Fig. 3.

macroscopic quantities was found even in the case of a strong condensation (see also Refs. [37–40]). This may be because a degree of the polynomial in the Garzó et al.'s model is lower than that of our polynomial model.

The data of numerical computations in Figs. 3–5 are summarized below. We first note that, since the correct value of p_∞/p_w for given T_∞/T_w, $M_{n\infty}$, $M_{t\infty}$, and Γ is not known beforehand [see Eq. (27) and footnote 3], we cannot obtain the numerical solution directly. Instead, we repeat the computation with various p_∞/p_w, until the uniform equilibrium state at the far field from the condensed phase is achieved. Then the final solution and correct p_∞/p_w will be obtained simultaneously. In the finite-difference method for the model equations, 600 nonuniform lattice points in $0 \leqslant X_1 \lesssim 80\ell_w$ (the lattice interval ΔX_1 is $7.4 \times 10^{-7}\ell_w$ at $X_1 = 0$ and $0.2\ell_w$ for sufficiently large X_1) were used in the case of $g_c = 0.9563$, and 800 points in $0 \leqslant X_1 \lesssim 240\ell_w$ ($\Delta X_1 = 9.4 \times 10^{-7}\ell_w$ at

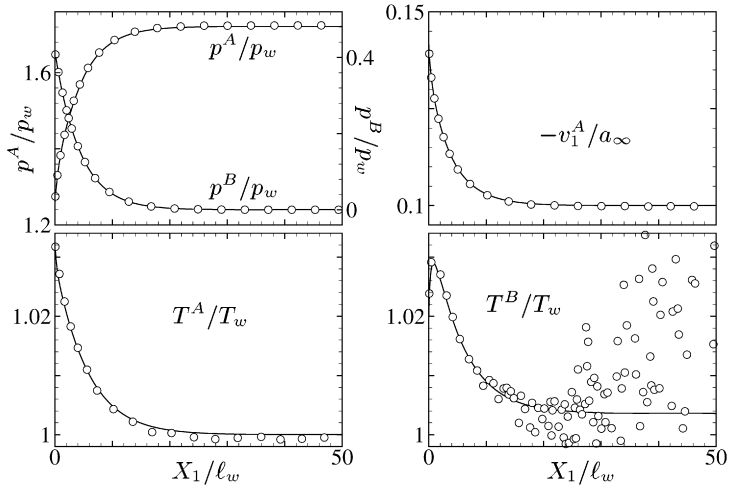

(a) $M_{t\infty} = 0$

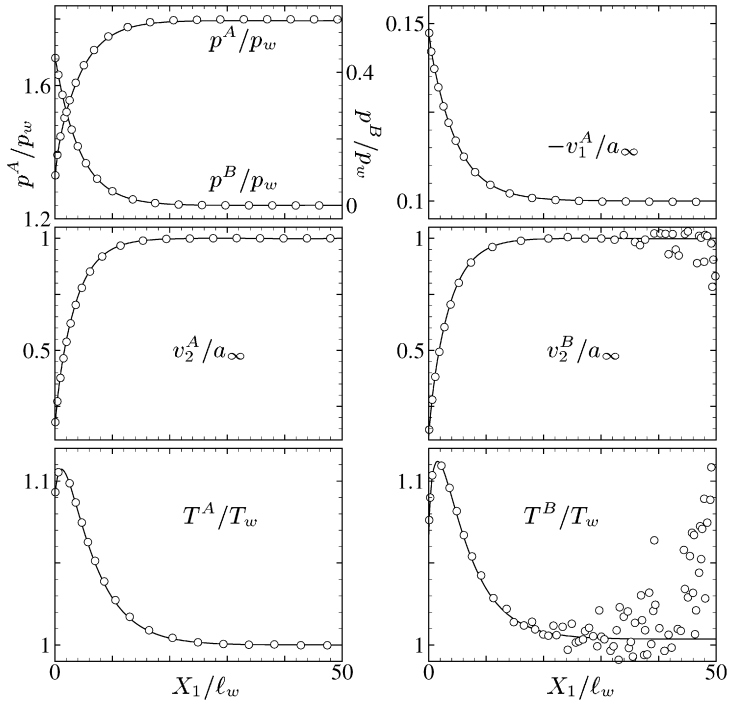

(b) $M_{t\infty} = 1$

Fig. 6. Profiles of the macroscopic quantities for $M_{n\infty} = 0.1$, $m^B/m^A = 1$, $d^B/d^A = 1$, and $\Gamma = 2$. (a) $M_{t\infty} = 0$, and (b) $M_{t\infty} = 1$. The —– indicates results of the polynomial model and ∘ those of the Boltzmann equation for hard-sphere molecules.

$X_1 = 0$ and $0.45\ell_w$ for sufficiently large X_1) in the case of $g_c = 2$. As for the molecular velocity, 209 nonuniform lattice points in $|\xi_1| \leqslant 5.6c_0$ with $c_0 = (2kT_0/m^A)^{1/2}$ were used ($\Delta\xi_1/c_0 = 5 \times 10^{-6}$ at $\xi_1 = 0$ and 0.16 at $|\xi_1| = 5.6c_0$). The typical CPU time including the repetition process to find the correct p_∞/p_w was $2 \sim 20$ hours on Intel Xeon 3.0 GHz processor. In the DSMC method for the Boltzmann equation, uniform cells with a length of $0.2\ell_w$ in $0 \leqslant X_1 \lesssim 80\ell_w$ were used in the case of $g_c = 0.9563$ and those with a length of $0.4\ell_w$ in $0 \leqslant X_1 \lesssim 240\ell_w$ in the case of $g_c = 2$. The total number of simulation particles in the final steady state was about $61\,000 \sim 82\,000$ for gas A and $500 \sim 1000$ for gas B. The time step was $0.01t_0$, where $t_0 = \ell_w/(2kT_w/m^A)^{1/2}$. The average of 1 000 000 samples with sampling interval $0.1t_0$ was taken to reduce the statistical scatter and the typical CPU time for this averaging process was $13 \sim 15$ hours. Such an averaging process had to be repeated several times to obtain the final solution with correct p_∞/p_w. Since the efficiency of the repetition toward correct p_∞/p_w is different for each numerical method, the CPU time advantage of a finite-difference calculation for the polynomial model over the DSMC for the Boltzmann equation is not very clear in this problem. However, the former calculation is surely advantageous in capturing the behavior of a component species with very small concentration (see the last sentence in the second paragraph in Section 4.1.2).

4.2. Case of the hard-sphere molecules

In this section, we make comparisons between the Boltzmann equation and the polynomial model introduced in Section 3.2 in the case of the hard-sphere (HS) molecular gases. First we consider the same half-space problem described in Section 4.1.1. Then we consider another fundamental problem, i.e., the two-surface

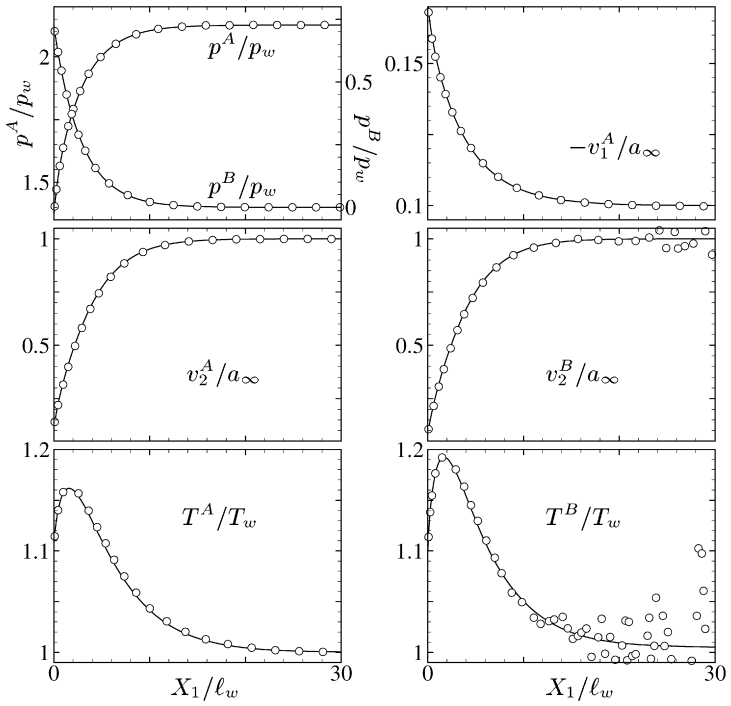

Fig. 7. Profiles of the macroscopic quantities for $M_{n\infty} = 0.1$, $M_{t\infty} = 1$, $m^B/m^A = 5$, $d^B/d^A = 1$, and $\Gamma = 2$. See the caption of Fig. 6.

problem of a vapor–gas mixture, because accurate numerical solutions of the Boltzmann equation for the HS molecules obtained by means of a finite-difference method are available.

4.2.1. Comparison in the half-space problem of a vapor and noncondensable gas

We first consider the same problem as described in Section 4.1.1 but in the case of the HS molecules. The parameter Γ here should be defined by Eq. (26) with $\ell_\infty = [\sqrt{2}\pi n_\infty (d^A)^2]^{-1}$. The problem is characterized by the following dimensionless parameters: T_∞/T_w, p_∞/p_w, $M_{n\infty}$, $M_{t\infty}$, m^B/m^A, d^B/d^A, and Γ. Here we restrict ourselves to the case of $T_\infty/T_w = 1$ and $d^B/d^A = 1$, and perform computations for various values of $M_{n\infty}$ (< 1), $M_{t\infty}$, m^B/m^A, and Γ ($\leqslant \Gamma_*$). Then the remaining p_∞/p_w is determined simultaneously with the solution so that Eq. (27) is satisfied. The Chapman–Cowling's Ω integrals contained in the polynomial model are given by Eq. (A.5) in Appendix A in the case of the HS molecule. As for the parameter $K_M^{\beta\alpha}$ appearing in the model, we employ the definition that was proposed in Ref. [45] for the McCormack model equation and is often used in literature (see, e.g., Refs. [35,36]). That is, noting that $K_M^{\beta\alpha}$ actually appears only in the form of K_M^α ($= K_M^{B\alpha} n^B + K_M^{A\alpha} n^A$) [see Eqs. (1), (21), (22a), and (A.1)], we define K_M^α as

$$
\begin{aligned}
&K_M^A = \frac{\Psi^A \Psi^B - n^A n^B \nu_{BA}^{(4)} \nu_{AB}^{(4)}}{\Psi^B + n^B \nu_{BA}^{(4)}}, \qquad K_M^B = K_M^A \frac{\Psi^B + n^B \nu_{BA}^{(4)}}{\Psi^A + n^A \nu_{AB}^{(4)}},\\
&\Psi^A = n^A \big(\nu_{AA}^{(3)} - \nu_{AA}^{(4)}\big) + n^B \nu_{BA}^{(3)},\\
&\Psi^B = n^B \big(\nu_{BB}^{(3)} - \nu_{BB}^{(4)}\big) + n^A \nu_{AB}^{(3)},
\end{aligned}
\tag{28}
$$

where $\nu_{\beta\alpha}^{(n)}$ is defined by Eq. (A.2) in Appendix A. The Boltzmann equation was solved by the DSMC method and the model by a finite-difference method.

Figs. 6 and 7, corresponding to Figs. 3–5 in the previous section, show profiles of the macroscopic quantities in the case of a relatively weak condensation ($M_{n\infty} = 0.1$): Fig. 6 is for $m^B/m^A = 1$ (i.e., molecules are mechanically identical) and Fig. 7 for $m^B/m^A = 5$. Here the space coordinate X_1 is normalized by the reference mean free path $\ell_w = [\sqrt{2}\pi n_w (d^A)^2]^{-1}$ with $n_w = p_w/kT_w$. The data of numerical computations in Figs. 6 and 7 are much the same as those in the case of the pseudo Maxwell molecule with $g_c = 0.9563$ (see the last paragraph in Section 4.1.2). We also performed computations for $M_{n\infty} = 0.5$ and 0.9 but omit their results because of the same reason as that in Section 4.1.2. However, it is seen in Figs. 6 and 7 that the polynomial model reproduces well results of the Boltzmann equation for the HS molecules when the condensation is weak.

4.2.2. Comparison in the two-surface problem of a vapor and noncondensable gas

We next consider the problem of a vapor (species A) and noncondensable gas (species B) between two parallel plane condensed phases of the vapor. The condensed phases are located at $X_1 = 0$ and D, and their temperatures are kept at T_I and T_II ($> T_\mathrm{I}$). The saturation number density of the vapor is n_I^A at temperature T_I and n_II^A at T_II. Then we investigate the steady flow of the vapor caused by evaporation and condensation and the behavior of the noncondensable gas. The boundary condition at the surface of the condensed phase is the complete condensation for the vapor (see footnote 2) and the diffuse reflection for the noncondensable gas. The problem is characterized by the following parameters: $T_\mathrm{II}/T_\mathrm{I}$, $n_\mathrm{II}^A/n_\mathrm{I}^A$, m^B/m^A, d^B/d^A, $n_\mathrm{av}^B/n_\mathrm{I}^A$, and Kn ($= \ell_0/D$), where n_av^B is the average number density of the noncondensable gas defined as

$$
n_\mathrm{av}^B = \frac{1}{D}\int_0^D n^B(X_1)\,\mathrm{d}X_1,
\tag{29}
$$

$\ell_0 = [\sqrt{2}\pi n_\mathrm{I}^A (d^A)^2]^{-1}$ the reference molecular mean free path, and Kn the Knudsen number.

The behavior of the mixture in the continuum limit (Kn $\to 0$) in this problem was investigated in Refs. [46–48] and the following facts were clarified: (i) the evaporation and condensation stop and the vapor flow vanishes as Kn $\to 0$ for fixed nonzero values of $n_\mathrm{av}^B/n_\mathrm{I}^A$ ($\neq 0$); (ii) the vapor flow continues to exist in the limit Kn $\to 0$ with $n_\mathrm{av}^B/n_\mathrm{I}^A = \Delta\mathrm{Kn}$ (Δ is a constant). In the case (i), the

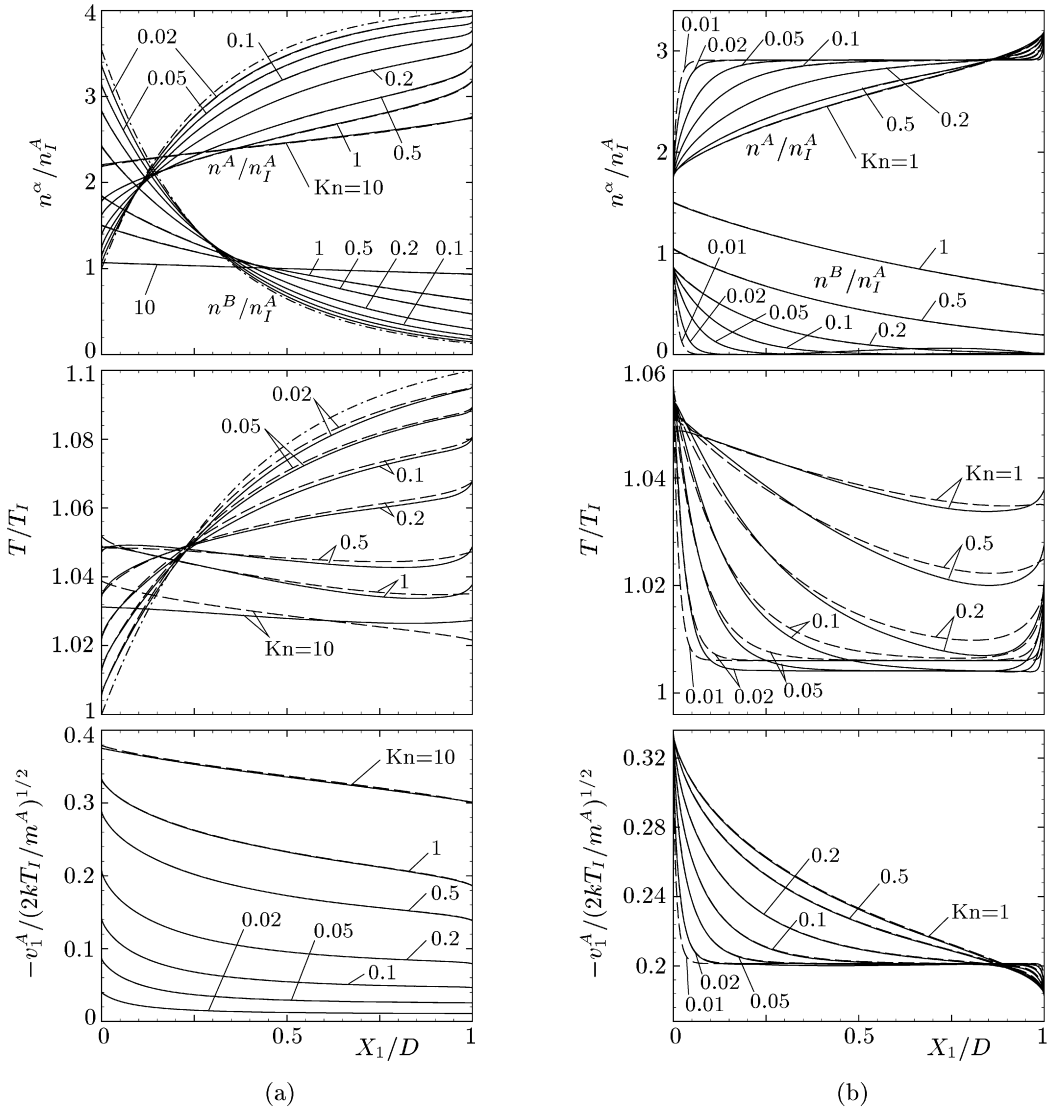

Fig. 8. Profiles of n^A, n^B, T, and v_1^A in the case of $T_{II}/T_I = 1.1$, $n_{II}^A/n_I^A = 4$, $m^B/m^A = 1$, and $d^B/d^A = 1$: (a) $n_{av}^B/n_I^A = 1$ and $0.02 \leqslant \mathrm{Kn} \leqslant 10$, and (b) $n_{av}^B/n_I^A = \mathrm{Kn}$ and $0.01 \leqslant \mathrm{Kn} \leqslant 1$ ($0.02 \leqslant \mathrm{Kn} \leqslant 1$ for the Boltzmann equation). The —— indicates results of the Boltzmann equation in Ref. [50], – – – those of the polynomial model, and – · – in (a) those of the Boltzmann equation in the continuum limit ($\mathrm{Kn} \to 0$).

infinitesimal vapor flow in the continuum limit exerts a finite influence on the behavior of the mixture in the same limit, which is an example of the *ghost effect* first revealed in Ref. [49] in the case of a single-component gas. In the case (ii), the behavior of the vapor flow in the continuum limit changes according to the value of Δ, which means that an infinitesimal amount of the noncondensable gas exerts a finite influence on the vapor flow.

Taking into account the findings in Refs. [46–48], Fig. 8(a) shows results for various values of Kn in the case of $n_{av}^B/n_I^A = 1$ and Fig. 8(b) in the case of $n_{av}^B/n_I^A = \mathrm{Kn}$ (i.e., $\Delta = 1$). Solutions of the Boltzmann equation and those of the model in the figure were obtained by means of a finite-difference method, respectively, in Ref. [50] and in the present work. The $K_M^{\beta\alpha}$ in the model was defined in the same manner as in Section 4.2.1. Although the profiles of T show remarkable differences, the polynomial model reproduces well profiles of the other quantities obtained by the Boltzmann equation (note that the ordinate in the figure of T is magnified compared with that in the other figures). In this problem, negative values of the velocity distribution function obtained by the model are found again but their absolute values are very small. In the finite-difference calculation of the model equation, 400 nonuniform lattice points for X_1 (the lattice interval is $6.3 \times 10^{-8} D$ at the boundaries and $7.5 \times 10^{-3} D$ at the center of the gap) were used in the case of $\mathrm{Kn} > 0.02$ and 800 points in the case of $\mathrm{Kn} \leqslant 0.02$; for ξ_1, the same lattice points as those in Section 4.1 were used. The CPU time of the calculation for the case of $\mathrm{Kn} = 0.02$ in Fig. 8(a), for example, was about 2 hours on a personal computer with Intel Xeon 3.0 GHz processor. On the other hand, calculations of the Boltzmann equation were carried out on the supercomputer Fujitsu VPP800/63 at the Data Processing Center, Kyoto University. The computing time for the same case was about 11 hours in a parallel computation using 40 CPU's. See Ref. [50] for details (the number of lattice points, etc.) of the finite-difference calculation of the Boltzmann equation.

5. Conclusions

The polynomial model for the nonlinear Boltzmann equation for gas mixtures was constructed by the method employed in the derivation of the McCormack model [20] in the linearized kinetic theory. It was compared numerically with the Boltzmann equation and with other existing models proposed by Andries, Aoki, and Perthame [18] and by Holway [4,5] (the so-called ES-BGK model).

As mentioned in Section 3.1, the Andries et al.'s model and ES-BGK model are basically appropriate for the Maxwell molecular gases, since the collision term of those two models is constructed so that its low order moments coincide with the counterparts of the Boltzmann equation for the Maxwell molecules shown in Section 2.1. On the other hand, the polynomial model can fit to general molecular models. The three model equations were, therefore, first compared with the Boltzmann equation for the pseudo Maxwell molecules (Section 4.1), and then only the polynomial model was compared with the Boltzmann equation for the hard-sphere (HS) molecules (Section 4.2). The comparison was mainly performed in the half-space problem of a vapor condensing onto a plane condensed phase in the presence of a noncondensable gas, after parameters contained in the models were adjusted appropriately. In the case of the HS molecule, the comparison in the two-surface problem of a vapor–gas mixture was also performed, since accurate numerical solutions of the Boltzmann equation obtained by a finite-difference method are available.

The results of the comparisons in Section 4.1 clearly indicate that the higher order moment of the model collision term coincides with that of the original one, the better resemblance between solutions of the Boltzmann equation and those of its model may be achieved. Indeed, the polynomial model best approximates solutions of the Boltzmann equation for the pseudo Maxwell molecules. It also reproduces well solutions of the Boltzmann equation for the HS molecules. However, although the polynomial model works well in the case of weakly nonequilibrium flows, it does not in the case of strongly nonequilibrium flows, since the positivity of the velocity distribution function is not assured. The latter case should be dealt with by the original Boltzmann equation. The applicability of the polynomial model, therefore, is limited, but still it might be an effective tool for the investigation of gas mixtures in some areas of studies (e.g. microfluidics). As mentioned in the fourth paragraph in Section 1, simulations based on the general molecular models other than the Maxwell molecular model could be important in studies on the behavior of gas mixtures.

Acknowledgements

The author expresses cordial thanks to Prof. K. Aoki and Prof. S. Takata for their valuable comments on the manuscript. This work was partially supported by the Center of Excellence for Research and Education on Complex Functional Mechanical Systems.

Appendix A. Expressions of $\Phi^{\beta\alpha}_{(1)i}$, $\Phi^{\beta\alpha}_{(2)}$, $\Phi^{\beta\alpha}_{(3)ij}$, and $\Phi^{\beta\alpha}_{(4)i}$

The coefficients $\Phi^{\beta\alpha}_{(1)i}$, $\Phi^{\beta\alpha}_{(2)}$, $\Phi^{\beta\alpha}_{(3)ij}$, and $\Phi^{\beta\alpha}_{(4)i}$ for the model equation in Section 3.2 determined by Eq. (23) may be written in the following forms:

$$\begin{aligned}\Phi^{\beta\alpha}_{(1)i} &= K^{\beta\alpha}_M n^\beta A^\alpha_i + \left(n^\alpha A^\beta_i\sqrt{\frac{m^\alpha}{m^\beta}} - n^\beta A^\alpha_i\right)\nu^{(1)}_{\beta\alpha} \\ &\quad + \left(\frac{n^\alpha D^\beta_i}{m^\beta}\sqrt{\frac{m^\alpha}{m^\beta}} - \frac{n^\beta D^\alpha_i}{m^\alpha}\right)\nu^{(2)}_{\beta\alpha} \\ &\quad + \left[\frac{5}{2}\left(\frac{A^\beta_i B^\alpha}{m^\alpha}\sqrt{\frac{m^\alpha}{m^\beta}} - \frac{B^\beta A^\alpha_i}{m^\beta}\right) + \frac{A^\beta_j C^\alpha_{ij}}{m^\alpha}\sqrt{\frac{m^\alpha}{m^\beta}} - \frac{C^\beta_{ij}A^\alpha_j}{m^\beta}\right]\nu^{(2)}_{\beta\alpha} \\ &\quad + \left[\frac{5}{2}\left(D^\beta_i B^\alpha\sqrt{\frac{m^\alpha}{m^\beta}} - B^\beta D^\alpha_i\right) + D^\beta_j C^\alpha_{ij}\sqrt{\frac{m^\alpha}{m^\beta}} - C^\beta_{ij}D^\alpha_j\right]\Upsilon^{(1)}_{\beta\alpha},\end{aligned} \tag{A.1a}$$

$$\begin{aligned}\Phi^{\beta\alpha}_{(2)} &= K^{\beta\alpha}_M n^\beta B^\alpha + \left(n^\alpha B^\beta - n^\beta B^\alpha\right)\frac{\mu^{\beta\alpha}}{m^\beta}\nu^{(1)}_{\beta\alpha} \\ &\quad + \frac{2}{3}\sqrt{\frac{m^\alpha}{m^\beta}}\left[A^\beta_k D^\alpha_k\left(3 - \frac{m^\beta}{m^\alpha}\right) - D^\beta_k A^\alpha_k\left(3 - \frac{m^\alpha}{m^\beta}\right)\right]\frac{\mu^{\beta\alpha}}{m^\beta m^\alpha}\nu^{(2)}_{\beta\alpha} \\ &\quad + \frac{4}{3}\frac{m^\beta - m^\alpha}{m^\beta + m^\alpha}\left[-A^\beta_k A^\alpha_k\sqrt{\frac{m^\alpha}{m^\beta}}\nu^{(1)}_{\beta\alpha}\right. \\ &\quad \left. + \frac{1}{2m^\beta}\left(\frac{15}{2}B^\beta B^\alpha + C^\beta_{kl}C^\alpha_{kl}\right)\nu^{(2)}_{\beta\alpha} - 3D^\beta_k D^\alpha_k\sqrt{\frac{m^\alpha}{m^\beta}}\Upsilon^{(1)}_{\beta\alpha}\right],\end{aligned} \tag{A.1b}$$

$$\begin{aligned}\Phi^{\beta\alpha}_{(3)ij} &= \left(K^{\beta\alpha}_M - \nu^{(3)}_{\beta\alpha}\right)n^\beta C^\alpha_{ij} + n^\alpha C^\beta_{ij}\nu^{(4)}_{\beta\alpha} \\ &\quad + \overline{A^\beta_i A^\alpha_j}\sqrt{\frac{m^\alpha}{m^\beta}}\Upsilon^{(2)}_{\beta\alpha} + \overline{A^\beta_i D^\alpha_j}\sqrt{\frac{m^\alpha}{m^\beta}}\Upsilon^{(3)}_{\beta\alpha} + \overline{A^\alpha_i D^\beta_j}\sqrt{\frac{m^\alpha}{m^\beta}}\Upsilon^{(4)}_{\beta\alpha} \\ &\quad + B^\beta C^\alpha_{ij}\Upsilon^{(5)}_{\beta\alpha} + C^\beta_{ij}B^\alpha\Upsilon^{(6)}_{\beta\alpha} + \overline{C^\beta_{il}C^\alpha_{jl}}\Upsilon^{(7)}_{\beta\alpha} + \overline{D^\beta_i D^\alpha_j}\sqrt{\frac{m^\alpha}{m^\beta}}\Upsilon^{(8)}_{\beta\alpha},\end{aligned} \tag{A.1c}$$

$$\begin{aligned}\Phi^{\beta\alpha}_{(4)i} &= \left(K^{\beta\alpha}_M - \nu^{(5)}_{\beta\alpha}\right)n^\beta D^\alpha_i + n^\alpha D^\beta_i\sqrt{\frac{m^\alpha}{m^\beta}}\nu^{(6)}_{\beta\alpha} \\ &\quad + \frac{5}{2m^\alpha}\left(n^\alpha A^\beta_i\sqrt{\frac{m^\alpha}{m^\beta}} - n^\beta A^\alpha_i\right)\nu^{(2)}_{\beta\alpha} + A^\beta_i B^\alpha\sqrt{\frac{m^\alpha}{m^\beta}}\Upsilon^{(9)}_{\beta\alpha} \\ &\quad + B^\beta A^\alpha_i\Upsilon^{(10)}_{\beta\alpha} + A^\beta_j C^\alpha_{ij}\sqrt{\frac{m^\alpha}{m^\beta}}\Upsilon^{(11)}_{\beta\alpha} + C^\beta_{ij}A^\alpha_j\Upsilon^{(12)}_{\beta\alpha} \\ &\quad + B^\beta D^\alpha_i\Upsilon^{(13)}_{\beta\alpha} + D^\beta_i B^\alpha\sqrt{\frac{m^\alpha}{m^\beta}}\Upsilon^{(14)}_{\beta\alpha} + C^\beta_{ij}D^\alpha_j\Upsilon^{(15)}_{\beta\alpha} \\ &\quad + D^\beta_j C^\alpha_{ij}\sqrt{\frac{m^\alpha}{m^\beta}}\Upsilon^{(16)}_{\beta\alpha}.\end{aligned} \tag{A.1d}$$

Here A^α_i, B^α, C^α_{ij}, and D^α_i are defined in Eq. (25) and the notation introduced in Eq. (14) was used. The $\nu^{(i)}_{\beta\alpha}$ $(i = 1, 2, \ldots, 6)$ are defined as follows:

$$\begin{aligned}&\nu^{(1)}_{\beta\alpha} = \frac{8}{3}\frac{\mu^{\beta\alpha}}{m^\alpha}\Omega^{\beta\alpha}_{11}, \qquad \nu^{(2)}_{\beta\alpha} = \frac{\mu^{\beta\alpha}}{5}\left(\frac{8}{3}\frac{\mu^{\beta\alpha}}{m^\alpha}\Omega^{\beta\alpha}_{12} - \frac{5}{2}\nu^{(1)}_{\beta\alpha}\right), \\ &\nu^{(3)}_{\beta\alpha} = \frac{\mu^{\beta\alpha}}{m^\alpha}\left(\frac{4}{5}\frac{\mu^{\beta\alpha}}{m^\alpha}\Omega^{\beta\alpha}_{22} + \frac{m^\alpha}{m^\beta}\nu^{(1)}_{\beta\alpha}\right), \qquad \nu^{(4)}_{\beta\alpha} = \frac{m^\alpha}{m^\beta}\left(2\nu^{(1)}_{\beta\alpha} - \nu^{(3)}_{\beta\alpha}\right), \\ &\nu^{(5)}_{\beta\alpha} = \frac{8}{15}\frac{(\mu^{\beta\alpha})^3}{m^\beta(m^\alpha)^2}\left[\Omega^{\beta\alpha}_{22} + \left(\frac{15}{4}\frac{m^\alpha}{m^\beta} + \frac{25}{8}\frac{m^\beta}{m^\alpha}\right)\Omega^{\beta\alpha}_{11}\right. \\ &\qquad \left. - \frac{1}{2}\frac{m^\beta}{m^\alpha}\left(5\Omega^{\beta\alpha}_{12} - \Omega^{\beta\alpha}_{13}\right)\right], \\ &\nu^{(6)}_{\beta\alpha} = \frac{8}{15}\frac{(\mu^{\beta\alpha})^3}{m^\beta(m^\alpha)^2}\left(-\Omega^{\beta\alpha}_{22} + \frac{55}{8}\Omega^{\beta\alpha}_{11} - \frac{5}{2}\Omega^{\beta\alpha}_{12} + \frac{1}{2}\Omega^{\beta\alpha}_{13}\right),\end{aligned} \tag{A.2}$$

where $\Omega^{\beta\alpha}_{ij}$'s are the Chapman–Cowling integrals [23] defined later in Eq. (A.4). The above $\nu^{(i)}_{\beta\alpha}$'s were originally introduced in the construction of the McCormack model for the linearized Boltzmann equation for gas mixtures (see Ref. [20]). Similarly, $\Upsilon^{(i)}_{\beta\alpha}$ $(i = 1, 2, \ldots, 16)$ are defined in terms of $\Omega^{\beta\alpha}_{ij}$'s as follows:

$$\Upsilon^{(1)}_{\beta\alpha} = \frac{8}{75}\frac{(\mu^{\beta\alpha})^3}{m^\beta(m^\alpha)^2}\left(\frac{35}{4}\Omega^{\beta\alpha}_{11} - 7\Omega^{\beta\alpha}_{12} + \Omega^{\beta\alpha}_{13}\right), \tag{A.3a}$$

$$\Upsilon^{(2)}_{\beta\alpha} = 2\left(\nu^{(3)}_{\beta\alpha} - \frac{m^\beta}{m^\alpha}\nu^{(4)}_{\beta\alpha}\right), \tag{A.3b}$$

$$\Upsilon^{(3)}_{\beta\alpha} = \frac{2\mu^{\beta\alpha}}{m^\alpha}\left[\left(\frac{9}{5} - \frac{m^\beta}{m^\alpha}\right)\frac{\nu^{(2)}_{\beta\alpha}}{m^\beta} - \frac{8}{25}\left(\frac{\mu^{\beta\alpha}}{m^\alpha}\right)^2\left(\frac{7}{2}\Omega^{\beta\alpha}_{22} - \Omega^{\beta\alpha}_{23}\right)\right], \tag{A.3c}$$

$$\Upsilon^{(4)}_{\beta\alpha} = \frac{m^\alpha}{m^\beta}\Upsilon^{(3)}_{\beta\alpha} - \frac{16}{5}\frac{\nu^{(2)}_{\beta\alpha}}{m^\beta}, \qquad \Upsilon^{(5)}_{\beta\alpha} = -\frac{5}{8}\left(\Upsilon^{(4)}_{\beta\alpha} + 4\frac{\nu^{(2)}_{\beta\alpha}}{m^\beta}\right), \tag{A.3d}$$

$$\Upsilon^{(6)}_{\beta\alpha} = \Upsilon^{(5)}_{\beta\alpha} + 3\frac{\nu^{(2)}_{\beta\alpha}}{m^\beta}, \qquad \Upsilon^{(7)}_{\beta\alpha} = \frac{4}{7}\left(\Upsilon^{(6)}_{\beta\alpha} - \frac{3}{2}\frac{\nu^{(2)}_{\beta\alpha}}{m^\beta}\right), \tag{A.3e}$$

$$\Upsilon^{(8)}_{\beta\alpha} = \frac{2}{5}\frac{\mu^{\beta\alpha}}{m^\alpha}\left[9\left(\frac{m^\alpha}{m^\beta}-1\right)\Upsilon^{(1)}_{\beta\alpha} + \frac{8}{25}\frac{(\mu^{\beta\alpha})^3}{m^\beta (m^\alpha)^2}\left(\frac{63}{4}\Omega^{\beta\alpha}_{22} - 9\Omega^{\beta\alpha}_{23} + \Omega^{\beta\alpha}_{24}\right)\right], \tag{A.3f}$$

$$\Upsilon^{(9)}_{\beta\alpha} = \frac{5}{2}\left(\nu^{(5)}_{\beta\alpha} - \frac{\mu^{\beta\alpha}}{m^\beta}\nu^{(1)}_{\beta\alpha}\right), \qquad \Upsilon^{(10)}_{\beta\alpha} = \frac{5}{2}\left(-\nu^{(6)}_{\beta\alpha} + \frac{\mu^{\beta\alpha}}{m^\beta}\nu^{(1)}_{\beta\alpha}\right), \tag{A.3g}$$

$$\Upsilon^{(11)}_{\beta\alpha} = \nu^{(5)}_{\beta\alpha} - \nu^{(3)}_{\beta\alpha}, \qquad \Upsilon^{(12)}_{\beta\alpha} = -\nu^{(6)}_{\beta\alpha} + \nu^{(4)}_{\beta\alpha}, \tag{A.3h}$$

$$\Upsilon^{(13)}_{\beta\alpha} = \frac{5}{12}\frac{\mu^{\beta\alpha}}{m^\beta}\left[\left(1-\frac{m^\alpha}{m^\beta}\right)\Upsilon^{(3)}_{\beta\alpha} + \frac{\mu^{\beta\alpha}}{m^\alpha}\left(1-\frac{9}{10}\frac{m^\alpha}{m^\beta}-\frac{19}{4}\frac{m^\beta}{m^\alpha}\right)\frac{\nu^{(2)}_{\beta\alpha}}{m^\beta} + \frac{4}{25}\left(\frac{\mu^{\beta\alpha}}{m^\alpha}\right)^3\left(-35\Omega^{\beta\alpha}_{12} + 19\Omega^{\beta\alpha}_{13} - 2\Omega^{\beta\alpha}_{14}\right)\right], \tag{A.3i}$$

$$\Upsilon^{(14)}_{\beta\alpha} = -\Upsilon^{(13)}_{\beta\alpha} + 5\frac{m^\beta - m^\alpha}{m^\beta + m^\alpha}\frac{\nu^{(2)}_{\beta\alpha}}{m^\beta}, \tag{A.3j}$$

$$\Upsilon^{(15)}_{\beta\alpha} = \frac{2}{5}\Upsilon^{(13)}_{\beta\alpha} - \frac{1}{4}\frac{m^\alpha}{m^\beta}\Upsilon^{(3)}_{\beta\alpha} + \frac{\mu^{\beta\alpha}}{2m^\alpha}\left(3\frac{m^\alpha}{m^\beta}-1\right)\frac{\nu^{(2)}_{\beta\alpha}}{m^\beta}, \tag{A.3k}$$

$$\Upsilon^{(16)}_{\beta\alpha} = -\frac{2}{5}\Upsilon^{(13)}_{\beta\alpha} - \frac{1}{4}\frac{m^\alpha}{m^\beta}\Upsilon^{(3)}_{\beta\alpha} - \frac{1}{5}\frac{\nu^{(2)}_{\beta\alpha}}{m^\beta}. \tag{A.3l}$$

The Chapman–Cowling integral $\Omega^{\beta\alpha}_{ij}$ is defined in terms of the function $B^{\beta\alpha}$ as (see Ref. [21])

$$\Omega^{\beta\alpha}_{ij}(T) = \int_0^\infty \exp(-y^2) y^{2j+2} \Lambda^{\beta\alpha}_i(y,T)\,\mathrm{d}y,$$
$$\Lambda^{\beta\alpha}_i(y,T) = 2\sqrt{\pi}\int_0^{\pi/2} B^{\beta\alpha}\left(\cos\theta, \sqrt{\frac{2kT(m^\beta+m^\alpha)}{m^\beta m^\alpha}}\,y\right) \times \left[1-\cos^i(\pi-2\theta)\right]\sin\theta\,\mathrm{d}\theta. \tag{A.4}$$

As indicated above, $\Omega^{\beta\alpha}_{ij}$'s are generally functions of the local temperature T of the mixture. In the case of the hard-sphere molecule, substituting Eq. (5) into Eq. (A.4), one obtains

$$\Omega^{\beta\alpha}_{ij} = \frac{1}{4}\left(\frac{\pi kT}{\mu^{\beta\alpha}}\right)^{1/2}(d^{\beta\alpha})^2\left[2-\frac{1+(-1)^i}{i+1}\right](j+1)!. \tag{A.5}$$

In the case of the pseudo Maxwell molecule, substituting Eq. (6) with the angular cutoff into Eq. (A.4) with $i=1$ and 2, one obtains

$$\Omega^{\beta\alpha}_{1j} = \frac{\chi^{\beta\alpha}}{2\sqrt{\pi}}\Gamma\left(j+\frac{3}{2}\right), \qquad \Omega^{\beta\alpha}_{2j} = \frac{\eta^{\beta\alpha}}{3\sqrt{\pi}}\Gamma\left(j+\frac{3}{2}\right), \tag{A.6}$$

with Γ being the Gamma function and $\chi^{\beta\alpha}$ and $\eta^{\beta\alpha}$ being defined in Eqs. (12) and (15) respectively. Substituting Eq. (A.6) into Eqs. (A.2) and (A.3), one obtains $\nu^{(2)}_{\beta\alpha} = 0$ and $\Upsilon^{(n)}_{\beta\alpha} = 0$ ($n = 1, 3, 4, 5, 6, 7, 8, 13, 14, 15, 16$).

Appendix B. Transport coefficients

Let us consider a binary gas mixture (composed of species A and B), and let μ be the viscosity, λ the thermal conductivity, D_{AB} the mutual diffusion coefficient, and k_T the thermo-diffusion ratio. The first approximations to those transport coefficients in the Chapman–Enskog method are shown below. In the case of the Boltzmann equation for the pseudo Maxwell molecules, we have

$$\mu = kT\frac{\gamma_1^{BA}(X^A)^2 + \gamma_1^{AB}(X^B)^2 + \gamma_2 X^A X^B}{\eta^{AA}\gamma_1^{BA}(X^A)^2 + \eta^{BB}\gamma_1^{AB}(X^B)^2 + \gamma_3 X^A X^B}, \tag{B.1a}$$

$$\gamma_1^{\beta\alpha} = \frac{(\mu^{\beta\alpha})^2}{m^\beta m^\alpha}\left(\chi^{\beta\alpha} + \frac{1}{2}\frac{m^\alpha}{m^\beta}\eta^{\beta\alpha}\right), \tag{B.1b}$$

$$\gamma_2 = \eta^{BB} + \eta^{AA} + \frac{(\mu^{BA})^2}{m^B m^A}(2\chi^{BA} - \eta^{BA}), \tag{B.1c}$$

$$\gamma_3 = \eta^{BB}\eta^{AA} + 2\frac{(\mu^{BA})^2}{m^B m^A}\chi^{BA}\eta^{BA}, \tag{B.1d}$$

$$\lambda = \frac{15}{4}k^2T\frac{\frac{\tau_1^{BA}}{m^A}(X^A)^2 + \frac{\tau_1^{AB}}{m^B}(X^B)^2 + \tau_2 X^A X^B}{\eta^{AA}\tau_1^{BA}(X^A)^2 + \eta^{BB}\tau_1^{AB}(X^B)^2 + \tau_3 X^A X^B}, \tag{B.2a}$$

$$\tau_1^{\beta\alpha} = \frac{1}{2}\frac{(\mu^{\beta\alpha})^3}{(m^\beta)^2 m^\alpha}\left[\eta^{\beta\alpha} + \frac{3}{4}\left(\frac{m^\alpha}{m^\beta} + 3\frac{m^\beta}{m^\alpha}\right)\chi^{\beta\alpha}\right], \tag{B.2b}$$

$$\tau_2 = \frac{\eta^{BB}}{m^A} + \frac{\eta^{AA}}{m^B} + \frac{(\mu^{BA})^3}{(m^B m^A)^2}(3\chi^{BA} - \eta^{BA}), \tag{B.2c}$$

$$\tau_3 = \eta^{BB}\eta^{AA} + 3\frac{(\mu^{BA})^4}{(m^B m^A)^2}\chi^{BA}\left[\frac{9}{16}\frac{(m^B - m^A)^2}{m^B m^A}\chi^{BA} + \eta^{BA}\right], \tag{B.2d}$$

$$D_{AB} = \frac{kT}{n\mu^{BA}\chi^{BA}}, \qquad k_T = 0, \tag{B.3}$$

where X^α ($\equiv n^\alpha/n$) is the concentration of species α and $\chi^{\beta\alpha}$ and $\eta^{\beta\alpha}$ are given by Eqs. (12) and (15) respectively. Completely the same expressions are derived in the case of the model equation introduced in Section 3.2 for the pseudo Maxwell molecules [i.e., the model with the Chapman–Cowling's Ω integrals defined by Eq. (A.6) in Appendix A].

In the case of the ES-BGK model, D_{AB}, k_T, and μ are given by Eqs. (B.3) and (B.1) with $\chi^{\beta\alpha}$ and $\eta^{\beta\alpha}$ being replaced by $\chi_M^{\beta\alpha}$ and $\eta_M^{\beta\alpha}$, while λ is given by

$$\lambda = \frac{5}{2}k^2T\frac{\frac{K_M^{BA}}{m^A}(X^A)^2 + \frac{K_M^{BA}}{m^B}(X^B)^2 + \tau_{2M}X^A X^B}{K_M^{AA}K_M^{BA}(X^A)^2 + K_M^{BB}K_M^{BA}(X^B)^2 + \tau_{3M}X^A X^B}, \tag{B.4a}$$

$$\tau_{2M} = \frac{K_M^{BB}}{m^A} + \frac{K_M^{AA}}{m^B}, \qquad \tau_{3M} = K_M^{BB}K_M^{AA} + (K_M^{BA})^2. \tag{B.4b}$$

In the case of the Andries et al.'s model, D_{AB} and k_T are given by Eq. (B.3) with χ^{BA} being replaced χ_M^{BA} and λ by Eq. (B.4), while μ is given by

$$\mu = kT\frac{K_M^{BA}(X^A)^2 + K_M^{BA}(X^B)^2 + \gamma_{2M}X^A X^B}{K_M^{AA}K_M^{BA}(X^A)^2 + K_M^{BB}K_M^{BA}(X^B)^2 + \gamma_{3M}X^A X^B}, \tag{B.5a}$$

$$\gamma_{2M} = K_M^{BB} + K_M^{AA}, \qquad \gamma_{3M} = K_M^{BB}K_M^{AA} + (K_M^{BA})^2. \tag{B.5b}$$

References

[1] G.A. Bird, Molecular Gas Dynamics and the Direct Simulation of Gas Flows, Oxford University Press, Oxford, 1994.
[2] P.L. Bhatnagar, E.P. Gross, M. Krook, A model for collision processes in gases. I. Small amplitude processes in charged and neutral one-component systems, Phys. Rev. 94 (1954) 511–525.
[3] P. Welander, On the temperature jump in a rarefied gas, Ark. Fys. 7 (1954) 507–553.
[4] L.H. Holway Jr., Approximation procedures for kinetic theory, Ph.D. Thesis, Harvard University, 1963.
[5] L.H. Holway Jr., New statistical models for kinetic theory: Methods of construction, Phys. Fluids 9 (1966) 1658–1673.
[6] P. Andries, P. Le Tallec, J.-P. Perlat, B. Perthame, The Gaussian-BGK model of Boltzmann equation with small Prandtl number, Eur. J. Mech. B/Fluids 19 (2000) 813–830.
[7] P. Andries, J.-F. Bourgat, P. Le Tallec, B. Perthame, Numerical comparison between the Boltzmann and ES-BGK models for rarefied gases, Comput. Methods Appl. Mech. Engrg. 191 (2002) 3369–3390.
[8] L. Mieussens, H. Struchtrup, Numerical comparison of Bhatnagar–Gross–Krook models with proper Prandtl number, Phys. Fluids 16 (2004) 2797–2813.

[9] Y. Zheng, H. Struchtrup, Ellipsoidal statistical Bhatnagar–Gross–Krook model with velocity-dependent collision frequency, Phys. Fluids 17 (2005) 127103.
[10] E.P. Muntz, A.A. Alexeenko, S.F. Gimelshein, A.D. Ketsdever, Y.-L. Han, M.P. Young, J.H. Park, C. Ngalande, N.P. Selden, R.H. Lee, Low speed nano/micro/meso-scale rarefied flows driven by temperature and pressure gradients, in: M.S. Ivanov, A.K. Rebrov (Eds.), Rarefied Gas Dynamics, Siberian Branch of the Russian Academy of Sciences, Novosibirsk, 2007, pp. 1085–1092.
[11] E.P. Gross, M. Krook, Model for collision processes in gases: Small-amplitude oscillations of charged two-component systems, Phys. Rev. 102 (1956) 593–604.
[12] L. Sirovich, Kinetic modeling of gas mixtures, Phys. Fluids 5 (1962) 908–918.
[13] T.F. Morse, Kinetic model equations for a gas mixture, Phys. Fluids 7 (1964) 2012–2013.
[14] B.B. Hamel, Kinetic model for binary gas mixtures, Phys. Fluids 8 (1965) 418–425.
[15] A. Oppenheim, Nonlinear model of Boltzmann's equations for a many-component gas, Phys. Fluids 8 (1965) 992–993.
[16] H. Oguchi, A kinetic model for a binary mixture and its application to a shock structure, in: C.L. Brundin (Ed.), Rarefied Gas Dynamics, vol. I, Academic Press, New York, 1967, pp. 745–758.
[17] V. Garzó, A. Santos, J.J. Brey, A kinetic model for a multicomponent gas, Phys. Fluids A 1 (1989) 380–383.
[18] P. Andries, K. Aoki, B. Perthame, A consistent BGK-type model for gas mixtures, J. Stat. Phys. 106 (2002) 993–1018.
[19] S. Kosuge, H. Mizuno, K. Aoki, Numerical investigation on models of the Boltzmann equation for gas mixtures, in: M.S. Ivanov, A.K. Rebrov (Eds.), Rarefied Gas Dynamics, Siberian Branch of the Russian Academy of Sciences, Novosibirsk, 2007, pp. 286–291.
[20] F.J. McCormack, Construction of linearized kinetic models for gaseous mixtures and molecular gases, Phys. Fluids 16 (1973) 2095–2105.
[21] S. Takata, H. Sugimoto, S. Kosuge, Gas separation by means of the Knudsen compressor, Eur. J. Mech. B/Fluids 26 (2007) 155–181.
[22] H. Sugimoto, S. Takata, S. Kosuge, Gas separation effect of the pump driven by the thermal edge flow, in: M.S. Ivanov, A.K. Rebrov (Eds.), Rarefied Gas Dynamics, Siberian Branch of the Russian Academy of Sciences, Novosibirsk, 2007, pp. 1158–1163.
[23] S. Chapman, T.G. Cowling, The Mathematical Theory of Non-Uniform Gases, third ed., Cambridge University Press, Cambridge, 1970.
[24] C. Cercignani, The Boltzmann Equation and Its Applications, Springer-Verlag, New York, 1988.
[25] Y. Sone, Molecular Gas Dynamics, Theory, Techniques, and Applications, Birkhäuser, Boston, 2007.
[26] E. Goldman, L. Sirovich, Equations for gas mixtures, Phys. Fluids 10 (1967) 1928–1940.
[27] E.L. Walker, B.S. Tanenbaum, Investigation of kinetic models for gas mixtures, Phys. Fluids 11 (1968) 1951–1954.
[28] H. Grad, On the kinetic theory of rarefied gases, Comm. Pure Appl. Math. 2 (1949) 331–407.
[29] G. Liu, A method for constructing a model form for the Boltzmann equation, Phys. Fluids A 2 (1990) 277–280.
[30] E.M. Shakhov, Approximate kinetic equations in rarefied gas theory, Fluid Dynamics 3 (1) (1968) 112–115.
[31] E.M. Shakhov, Generalization of the Krook kinetic relaxation equation, Fluid Dynamics 3 (5) (1968) 95–96.
[32] B.M. Segal, J.H. Ferziger, Shock-wave structure using nonlinear model Boltzmann equations, Phys. Fluids 15 (1972) 1233–1247.
[33] T. Abe, H. Oguchi, A hierarchy kinetic model and its applications, in: J.L. Potter (Ed.), Rarefied Gas Dynamics, vol. II, AIAA, New York, 1977, pp. 781–793.
[34] J.H. Ferziger, H.G. Kaper, Mathematical Theory of Transport Processes in Gases, North-Holland Publishing Company, Amsterdam, 1972.
[35] F. Sharipov, D. Kalempa, Gaseous mixture flow through a long tube at arbitrary Knudsen numbers, J. Vac. Sci. Technol. A 20 (2002) 814–822.
[36] S. Kosuge, S. Takata, Database for flows of binary gas mixtures through a plane microchannel, Eur. J. Mech. B/Fluids 27 (2008) 444–465.
[37] Y. Sone, K. Aoki, T. Doi, Kinetic theory analysis of gas flows condensing on a plane condensed phase: Case of a mixture of a vapor and a noncondensable gas, Transp. Theory Stat. Phys. 21 (1992) 297–328.
[38] K. Aoki, T. Doi, High-speed vapor flows condensing on a plane condensed phase in the presence of a noncondensable gas, in: B.D. Shizgal, D.P. Weaver (Eds.), Rarefied Gas Dynamics: Theory and Simulations, AIAA, Washington, DC, 1994, pp. 521–536.
[39] S. Taguchi, K. Aoki, S. Takata, Vapor flows condensing at incidence onto a plane condensed phase in the presence of a noncondensable gas. I. Subsonic condensation, Phys. Fluids 15 (2003) 689–705.
[40] S. Taguchi, K. Aoki, S. Takata, Vapor flows condensing at incidence onto a plane condensed phase in the presence of a noncondensable gas. II. Supersonic condensation, Phys. Fluids 16 (2004) 79–92.
[41] S. Taguchi, K. Aoki, V. Latocha, Vapor flows along a plane condensed phase with weak condensation in the presence of a noncondensable gas, J. Stat. Phys. 124 (2006) 321–369.
[42] Y. Sone, Kinetic theory of evaporation and condensation – linear and nonlinear problems, J. Phys. Soc. Jpn. 45 (1978) 315–320.
[43] S. Takata, Half-space problem of weak evaporation and condensation of a binary mixture of vapors, in: M. Capitelli (Ed.), Rarefied Gas Dynamics, AIP, New York, 2005, pp. 503–508.
[44] S. Takata, F. Golse, Half-space problem of the nonlinear Boltzmann equation for weak evaporation and condensation of a binary mixture of vapors, Eur. J. Mech. B/Fluids 26 (2007) 105–131.
[45] C. Cercignani, F. Sharipov, Gaseous mixture slit flow at intermediate Knudsen numbers, Phys. Fluids A 4 (1992) 1283–1289.
[46] K. Aoki, S. Takata, S. Kosuge, Vapor flows caused by evaporation and condensation on two parallel plane surfaces: Effect of the presence of a noncondensable gas, Phys. Fluids 10 (1998) 1519–1533.
[47] S. Takata, K. Aoki, T. Muraki, Behavior of a vapor–gas mixture between two parallel plane condensed phases in the continuum limit, in: R. Brun, R. Campargue, R. Gatignol, J.-C. Lengrand (Eds.), Rarefied Gas Dynamics, vol. 1, Cépaduès-Éditions, Toulouse, 1999, pp. 479–486.
[48] S. Takata, K. Aoki, Two-surface problems of a multicomponent mixture of vapors and noncondensable gases in the continuum limit in the light of kinetic theory, Phys. Fluids 11 (1999) 2743–2756.
[49] Y. Sone, K. Aoki, S. Takata, H. Sugimoto, A.V. Bobylev, Inappropriateness of the heat-conduction equation for description of a temperature field of a stationary gas in the continuum limit: Examination by asymptotic analysis and numerical computation of the Boltzmann equation, Phys. Fluids 8 (1996) 628–638; Erratum: Phys. Fluids 8 (1996) 841.
[50] K. Aoki, S. Kosuge, Finite-difference methods for the Boltzmann equation for binary gas mixtures, in: P. Degond, L. Pareschi, G. Russo (Eds.), Modeling and Computational Methods for Kinetic Equations, Birkhäuser, Boston, 2004, pp. 147–167.